Final Technical Report

THE FLOW OF PLASMA IN THE SOLAR TERRESTRIAL ENVIRONMENT

By: R.W. Schunk, P.I.
Center for Atmospheric and Space Sciences
Utah State University
Logan, Utah 84322-4405

Co-Investigators:

P. Banks
A.R. Barakat
D. J. Crain
H.G. Demars
J. Lemaire
T.-Z. Ma
C.E. Rasmussen
P. Richards
R. Sica
N. Singh
J.J. Sojka
J.-P. St.-Maurice
H. Thiemann
D. Torr
W.-H. Yang
L. Zhu

For: T.J. Birmingham
Code 695
Solar Terrestrial Theory Program
NASA/Goddard Space Flight Center
Greenbelt, Maryland 20771

Grant: NAGW-77

Period: 1 July 1980 – 30 September 1990

INTRODUCTION

It has been clearly established, both experimentally and theoretically, that the various regions of the solar-terrestrial system are *strongly coupled*, that the coupling processes exhibit *time delays*, and that *feedback* mechanisms exist [cf. *Intriligator*, 1984; *Romick et al.*, 1987; *Liu and Edwards*, 1988; *Roederer*, 1988; *Schunk*, 1989]. For example, changes in the solar wind dynamic pressure and the interplanetary magnetic field affect the magnetospheric currents and electric fields, which in turn, affect the ionospheric convection pattern, electron density morphology, and ion composition at high latitudes. The changes in the ionosphere then affect the thermospheric structure, circulation, and temperature on a global scale. The changes in the ionosphere-thermosphere system then act to modify the magnetospheric processes. The variations in the ionospheric conductivities modify the magnetospheric electric fields and the large-scale current system linking the two regions. Additional feedback mechanisms occur in the polar cap via the 'polar wind' and in the auroral zone via 'energetic ion outflow,' and these ionospheric ions are a significant source of mass, momentum, and energy for the magnetosphere. However, all of the coupling and feedback mechanisms have time delays associated with them, which further complicates the situation.

With the above description in mind, the overall goal of our NASA Theory Program was to study the *coupling, time delays,* and *feedback mechanisms* between the various regions of the solar-terrestrial system in a *self-consistent, quantitative* manner. To accomplish this goal, it will eventually be necessary to have time-dependent macroscopic models of the different regions of the solar-terrestrial system and we are continually working toward this goal. However, with the funding from this NASA program, we concentrated on the near-earth plasma environment, including the ionosphere, the plasmasphere, and the polar wind. In this area, we developed *unique global models* that allowed us to study the coupling between the different regions. These results are highlighted in the next section.

Another important aspect of our NASA Theory Program concerned the effect that localized 'structure' had on the macroscopic flow in the ionosphere, plasmasphere, thermosphere, and polar wind. The localized structure can be created by structured magnetospheric inputs (i.e., structured plasma convection, particle precipitation or Birkeland current patterns) or time variations in these inputs due to storms and substorms. Also, some of the plasma flows that we predicted with our macroscopic models could be unstable, and another one of our goals was to examine the stability of our predicted flows.

Because time-dependent, three-dimensional numerical models of the solar-terrestrial environment generally require extensive computer resources, they are usually based on relatively simple mathematical formulations (i.e., simple MHD or hydrodynamic formulations). Therefore, another goal of our NASA Theory Program was to study the conditions under which various mathematical formulations can be applied to specific solar-terrestrial regions. This could involve a detailed comparison of kinetic, semi-kinetic, and hydrodynamic predictions for a given polar wind scenario or it could involve the comparison of a small-scale particle-in-cell (PIC) simulation of a plasma expansion event with a similar macroscopic expansion event. The different mathematical formulations have different strengths and weaknesses and a careful comparison of model predictions for similar geophysical situations provides insight into when the various models can be used with confidence.

RESEARCH HIGHLIGHTS

As a result of our involvement in the NASA STTP program, we published 135 scientific papers and we presented 161 talks at both national and international meetings. These publications and presentations are listed at the back of this report. Because of the large number of publications, it is not possible to review all of our work in this final report. However, in the paragraphs that follow, we *highlight some* of the studies we conducted, with the emphasis on the work done during the last 3-5 years of the program.

Global Ionosphere

With support from the NASA Theory Program, we developed the *first* numerical model of the global ionosphere (papers 64, 107, 109, 112, 126, and 133). The model is a time-dependent, three-dimensional, high-resolution, multi-ion ionospheric model that covers the altitude range from 90–1000 km. With the model, the density distribution of six ion species (NO^+, O_2^+, N_2^+, O^+, N^+, He^+) and the electron and ion temperatures are obtained from a numerical solution of the appropriate continuity, momentum, and energy equations.

In recent work (paper 126), the global model was used to study the asymmetry in large-scale ionospheric features between the northern and southern hemispheres. The comparisons were done for June and December solstice conditions at solar maximum for quiet geomagnetic activity. Ideal conditions and diurnally-reproducible ionospheric features were established in order to elucidate the intrinsic hemispherical differences that are associated with the different displacements between the geomagnetic and geographic poles and the different atmospheric conditions. In comparing the ionospheric densities in the northern and southern hemispheres for a given season, we found the following: (1) The winter hemispheres display the most marked universal time (UT) variations due to the displacement between the geomagnetic and geographic poles; (2) For similar winter conditions, the electron densities in the northern and southern hemispheres can differ by an order of magnitude in places at certain UTs; (3) The winter mid-latitude trough is the feature that exhibits the largest northern-southern hemisphere difference due to the different dipole tilts; and (4) The 'winter anomaly' is present in the northern hemisphere at almost all UTs, while it is essentially absent in the southern hemisphere. In the northern hemisphere, the anomaly maximizes between 1000 and 1600 UT, with the winter/summer peak electron density (N_mF_2) ratio reaching 1.6. In our model, the anomaly results primarily from the adopted atmospheric densities.

Some of the hemispherical differences described above are shown in Figure 1, where contours of N_e at 300 km are displayed for one particular geometry of solar illumination. In the left panel, 1900 UT *June solstice* conditions are shown, while the right panel corresponds to 0700 UT *December solstice* conditions plotted with an inverted latitude axis. The latitude axis was inverted so that summer is at the top and winter at the bottom for both the northern and southern hemispheres.

Global Polar Wind

The polar wind is an ambipolar outflow of thermal plasma from the terrestrial ionosphere at high latitudes. The outflow typically begins at about 800 km. As the ionospheric ions flow up and out of the topside ionosphere along diverging geomagnetic

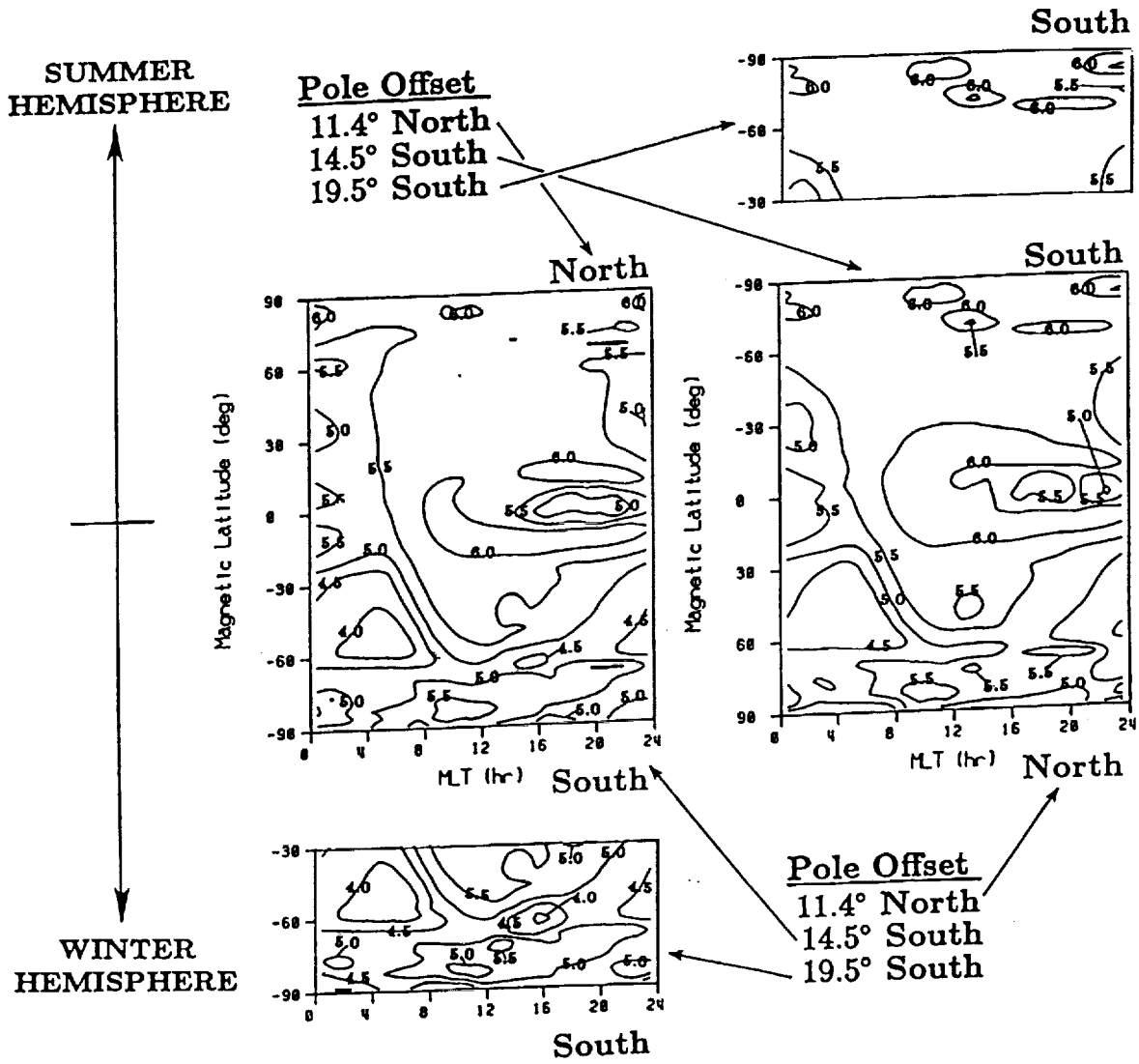

Figure 1. Global plot of the electron density variation at 300 km in a magnetic latitude-MLT reference frame. The left panels are for June solstice at 1900 UT and the right panels are for December solstice at 0700 UT. The top half of the figure is for the summer hemisphere and the bottom half is for the winter hemisphere. The two smaller panels show the N_e variation at 300 km in the southern hemisphere for a larger offset between the magnetic and geographic poles. The Ne contours are labeled in $\log_{10} N_e$ (cm^{-3}). From Paper 126.

field lines, they are accelerated and eventually become supersonic (above about 1300 km). Although the classical polar wind had been studied for twenty years, all of the studies were based on either steady state or time-dependent, one-dimensional models applied to a *single location*. However, we constructed the *first* three-dimensional, time-dependent, multi-ion model of the global polar wind in order to study the temporal evolution of ion outflow during magnetic storms and substorms (paper 130). The model covers the altitude range from 120 to 9000 km. At low altitudes (120–800 km), three-dimensional distributions for the NO^+, O_2^+, N_2^+, N^+, and O^+ densities and the ion and electron temperatures are obtained from a numerical solution of the appropriate continuity, momentum, and energy equations. At high altitudes (500–9000 km), the time-dependent, nonlinear, hydrodynamic equations for O^+ and H^+ are solved self-consistently with the ionospheric equations taking into account collisions, charge exchange chemical reactions, flux tube divergence, and ion temperature anisotropies. The model can describe supersonic ion outflow, shock formation, and ion energization during plasma expansion events.

In the first application of the model, we studied the temporal response of the global polar wind to changing magnetospheric conditions. During the simulation, the magnetic activity level changed from quiet to active and then back to quiet again over a 4.5-hour period. When the activity level increased, the auroral oval expanded, particle precipitation became more intense, and the convection electric field strengths increased. The reverse occurred during declining magnetic activity. From this study we found the following: (1) Plasma pressure changes in the ionosphere due to T_e, T_i, or electron density variations produce perturbations in the polar wind. In particular, plasma flux tube motion through the auroral oval and high electric field regions produces transient large-scale ion upflows and downflows. At certain times and in certain regions both inside and outside the auroral oval, H^+ –O^+ counterstreaming can occur; (2) The density structure in the polar wind is considerably more complicated than in the ionosphere because of both horizontal plasma convection and changing vertical propagation speeds due to spatially varying ionospheric temperatures; (3) During increasing magnetic activity, there is an overall increase in T_e, T_i, and the electron density in the F region, but there is a time delay in the buildup of the electron density that is as long as five hours at high altitudes; (4) During increasing magnetic activity, there is an overall increase in the polar wind outflow from the ionosphere, while the reverse is true for declining activity. In certain regions, however, localized ionospheric holes can develop during increasing magnetic activity, and in these locations the polar wind outflow rate is reduced; and (5) During changing magnetic activity, the temporal evolution of the ion density morphology at high altitudes (~ 9000 km) can be opposite to that at low altitudes (~ 500 km).

Some of these results are seen in Figure 2, which shows 'snapshots' of the H^+ density ($\log_{10}n$) at 500 km (bottom row), 2500 km (middle row) and 9000 km (top row) above the polar region for times corresponding to increasing activity (t_1), high activity (t_4), and declining activity (t_6). At the start of increasing magnetic activity (t_1), the H^+ density morphology is similar to the O^+ morphology (not shown), with relatively high densities in the oval in the midnight-dawn-noon sector, moderate densities in the central polar cap, and low densities in the dayside trough region. This result is not surprising, since at low altitudes O^+ is the source of H^+ via the $O^+ + H \Leftrightarrow H^+ + O$ reaction. As the storm intensifies (t_4), there is a large-scale H^+ upwelling that occurs in association with both the electron heating in the auroral oval due to increased particle precipitation and the ion heating in the regions of large electric fields. During declining magnetic activity (t_6), the H^+ density at 500 km is generally higher than what it was at any time during the storm. This time delay in the H^+ density buildup at low altitudes is simply a consequence of the time delay in the O^+ density buildup (not shown). However, at 2500 km, there are some polar regions where the H^+ density is lower than at the storm's main phase (t_4) and other polar

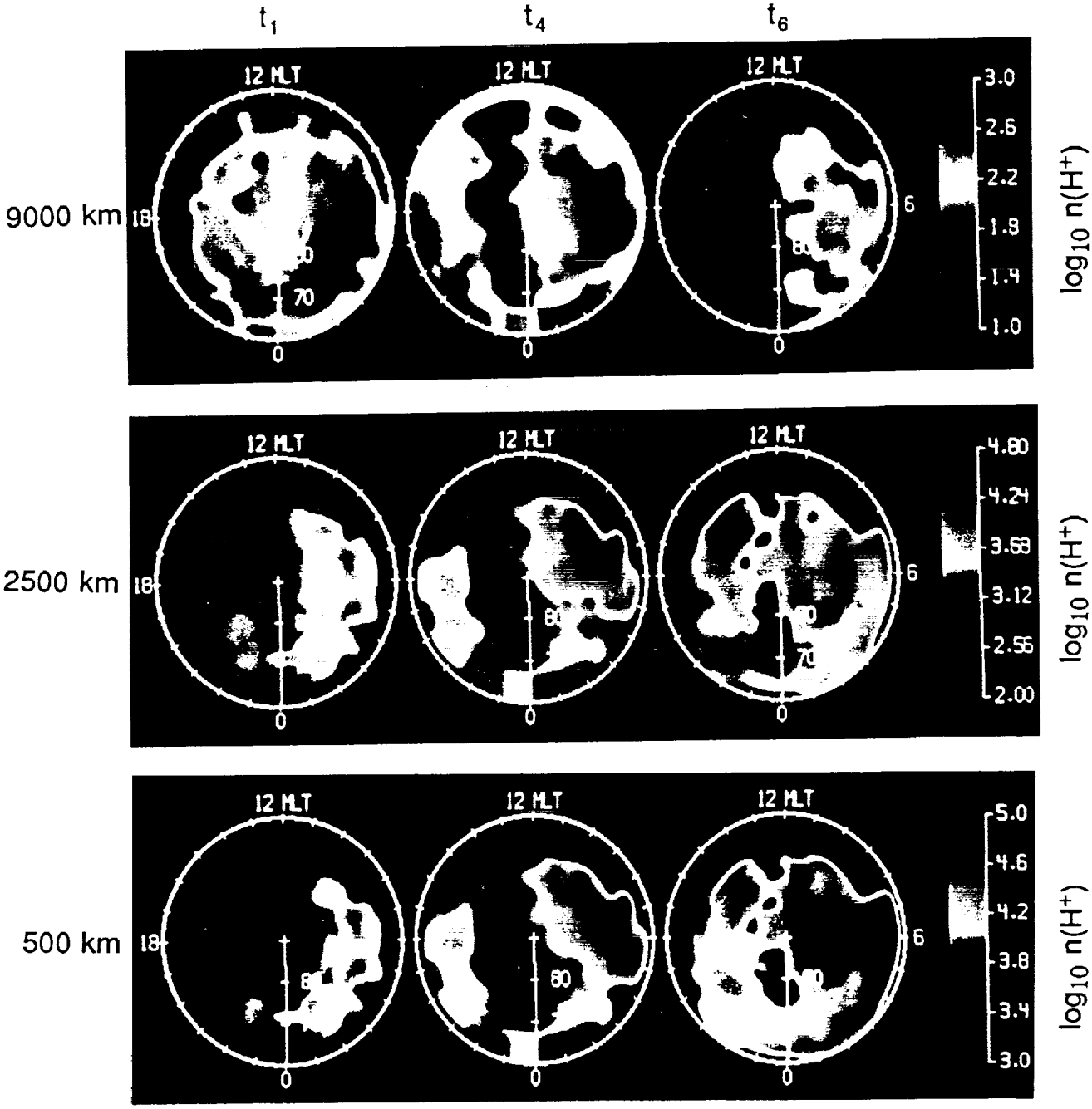

Figure 2. H+ density contours at 500 km (bottom row), 2500 km (middle row) and 9000 km (top row) for times corresponding to increasing (t_1), high (t_4) and declining (t_6) magnetic activity. A magnetic latitude-MLT reference frame is used. Note that different color scales are associated with the different altitudes. From paper 130.

regions where it is higher. Furthermore, at high altitudes (9000 km), there is an overall reduction in the H^+ density at t_6 relative to the storm's main phase (t_4) even though there is an overall H^+ density increase at low altitudes (500 km). The reason for the difference in the H^+ density morphologies at high and low altitudes during changing magnetospheric conditions is that there is a finite propagation time for low-altitude perturbations to reach high altitudes. The situation is further complicated by horizontal plasma convection, changing vertical propagation speeds with changing plasma temperatures, and localized regions where H^+ downflows can occur.

Global Plasmasphere

During the past two decades there have been several theoretical investigations of the coupling between thermal plasmas in the ionosphere and plasmasphere [e.g., *Horwitz*, 1983; *Lemaire*, 1985; and references therein]. Yet, there remains many unresolved questions in fundamental areas of research relating to the plasmasphere. An example of one of these areas is the location of the plasmapause. In spite of the obvious importance of the plasmapause, there remains an uncertainty as to the physical processes involved in its formation and location. For many years it has been accepted that the location of the plasmapause is controlled by a dynamic process associated with $\mathbf{E} \times \mathbf{B}$ convection in the magnetosphere [e.g., *Nishida*, 1966; *Brice*, 1967]. However, *Lemaire* [1985] has listed several problems with this model.

In order to study ionosphere-plasmasphere coupling phenomena and plasmapause formation mechanisms, we developed a three-dimensional, time-dependent model of the *global* plasmasphere. The model solves the nonlinear hydrodynamic continuity and momentum equations along closed flux tubes for *multiple* H^+ *streams* arising from the conjugate hemispheres. The model takes into account the production and loss of H^+, collisions of H^+ with O^+, and the motion of plasmaspheric flux tubes in response to convection electric fields (cross-L drifts). The model retains the inertial term in the momentum equation so that supersonic flow and various low frequency wave phenomena can be studied.

In our first study of the global plasmasphere (paper 132), the model was run for solar minimum conditions until diurnally reproducible results were obtained, indicating that the plasmasphere was fully filled. Equatorial densities obtained during this study are shown in the top panel of Figure 3. An interesting feature seen is the diurnal variation in density. Earthward of approximately $L = 2.5$, a minimum in density occurs at local midnight due to decreasing ionization levels in the ionosphere. However, the density of plasma near the plasmapause maximizes at local midnight due to a compression of the plasma as flux tubes convect toward the Earth in this time sector. The effect of expansion of the plasma can be seen in the dusk region, where the density of plasma convecting near the plasmapause is a minimum. Another view of the global plasmasphere is seen in the bottom panel of Figure 3, where H^+ densities are shown in the dusk-dawn meridian plane. This panel clearly shows the dusk bulge, indicated by the increased volume of the plasmasphere in the dusk sector relative to the dawn sector. When the results of the global model were compared with applicable measurements, it was found that the model results were within a factor of two of both the whistler and satellite observations. Near the plasmapause, changes in flux-tube volume due to cross-L drifts led to a factor of 3 variation in equatorial density, with the highest densities occurring near local midnight where the flux-tube volume was lowest.

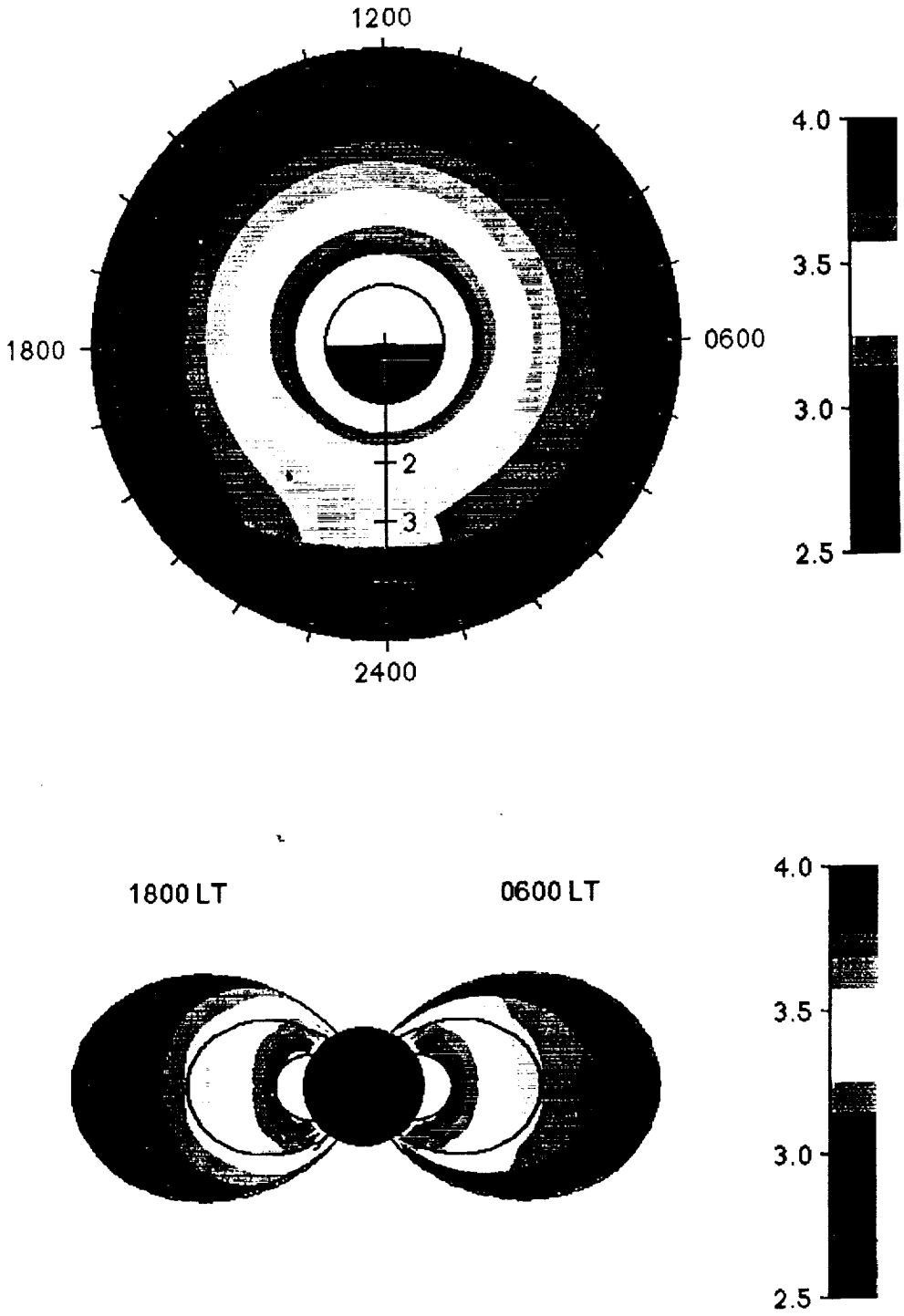

Figure 3. Contours of H^+ density in the equatorial plane of the magnetosphere (top). L value is indicated on the radial axis and local time on the outer circle. Sunlit and dark portions of the Earth are shown in the center of the figure. In the bottom panel, contours of H^+ density in the plasmasphere are shown at two different times. Black lines are plotted at L-shells of 1.5 and 3.0 and the outer red line is plotted at $L = 5.0$. The Earth is shown in light blue in the center. For both panels, the color scale is $\log_{10} n(H^+)$ in cm^{-3} and portions of the figure shown in black represent the plasma trough region outside of the plasmasphere. From Paper 132.

Polar Electrodynamics

In studies involving numerical simulations of the ionosphere, polar wind, plasmasphere, and thermosphere, the magnetospheric processes (field-aligned currents, convection electric fields, and particle precipitation) are usually taken as known inputs [cf. *Roble et al.*, 1988; *Fuller-Rowell and Rees*, 1983; papers 109, 130, 132, and 133]. These inputs are obtained from either empirical models or direct measurements. However, the field-aligned currents that flow into and out of the ionosphere are connected via horizontal currents that flow in the lower ionosphere (*E* region). These large-scale currents, the auroral conductivity enhancements due to precipitating energetic electrons (upward currents), and the convection electric fields are not independent, but instead, are related via Ohm's law and the current continuity equation. In this regard, we obtained a numerical solution of the appropriate equations in order to study the current-conductivity-electric field coupling between the ionosphere and magnetosphere (papers 95, 111, and 116). Our polar electrodynamics model is similar to the models developed earlier by others [cf. *Kamide et al.*, 1986; *Ahn et al.*, 1986; *Richmond and Kamide*, 1988]. With a measured field-aligned current distribution and conductivities calculated from our global ionospheric model, we are able to calculate the self-consistent convection electric fields and horizontal *E* region currents. We are also able to take into account the *F* region contribution to the ionospheric conductivity.

The current-conductivity-electric field coupling at high latitudes is strongly dependent on the direction of the interplanetary magnetic field (IMF). When the IMF is southward, the polar region is characterized by a two-cell pattern of plasma convection, Region 1 and 2 field-aligned current systems, and enhanced conductivities in the auroral oval. The overall consistency of these features is shown in Figure 4, where ionospheric conductivities, electric potentials, field-aligned currents, and *E* region currents are shown for one of our model simulations with $B_z < 0$ and $B_y < 0$ (paper 116). For northward IMF, on the other hand, the situation is more complicated and our work on this subject will be discussed later.

Large-Scale Ionospheric Structures

During the last decade, significant progress has been made in understanding the formation and evolution of the major morphological features observed in the high latitude ionosphere. However, the ionosphere exhibits a considerable amount of spatial structure that is not reproduced with the global numerical models when 'fixed' empirical models are adopted for the magnetospheric convection and precipitation patterns. There are small-scale ($\lesssim$ 1 km), medium-scale (~ 10 km), and large-scale ($\gtrsim$ 100 km) density structures [cf. *Buchau et al.*, 1985; *Weber et al.*, 1986; *Robinson et al.*, 1985; *Tsunoda*, 1988]. The small-scale structures appear to be produced within and on the edges of the larger structures through plasma instabilities and are typically referred to as density irregularities [*Kelley et al.*, 1982; *Lee*, 1984]. The medium and large-scale density structures have been called 'blobs', 'patches', and 'enhancements'. Relative to background densities, the perturbations associated with the medium and large-scale structures vary from about 10% to a factor of 100.

With regard to the medium and large-scale density structures, numerous structuring mechanisms have been proposed, including structured precipitation, structured electric fields, structured heat flow, transport from distant sources, structured enhanced decay, as well as time varying processes of all kinds [cf. *Kelley et al.*, 1982; *Heelis et al.*, 1986; *de la Beaujardiere et al.*, 1985; *Weber et al.*, 1984; *Robinson et al.*, 1985; paper 119]. Although all of the proposed mechanisms can produce density structures in a qualitative sense, very

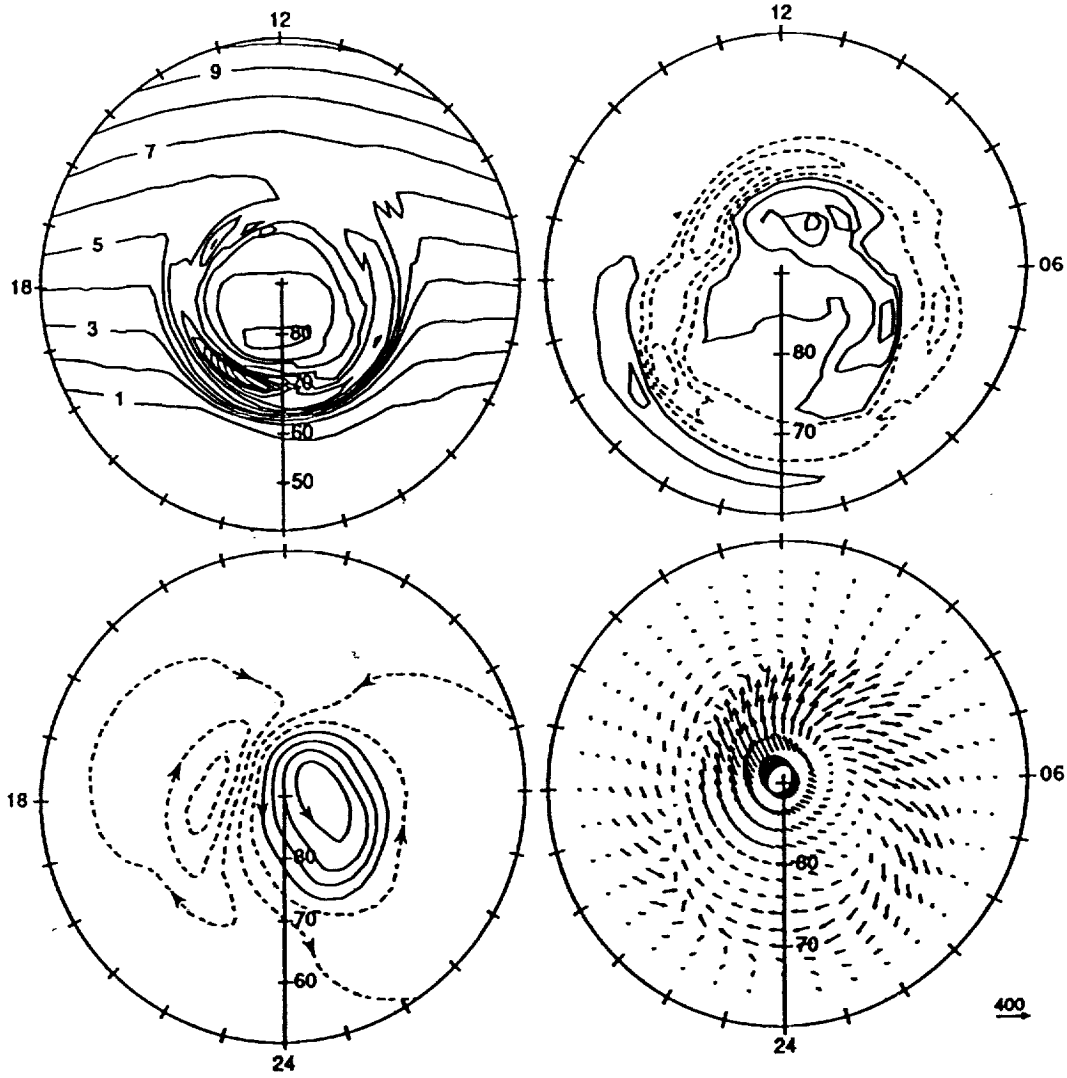

Figure 4. Pedersen conductivity (top left panel), Birkeland currents (top right panel), ionospheric electric potential (bottom left panel) and ionospheric currents (bottom right panel) for $B_z < 0$ and $B_y < 0$. The difference between contour levels is 0.1 mho for the conductivity plot. For the Birkeland currents, current flowing into the ionosphere is denoted by solid lines, while current flowing away from the ionosphere is shown by dashed lines (the contour separation is 0.2 μA/m^2). For the electric potential, solid lines denote positive potentials and dashed lines denote negative potentials (the contour separation is 6 kV). For the horizontal current, the vector scale is 400 A/km. From Paper 116.

little attention has been given to detailed quantitative studies of structure formation mechanisms. However, it is important to understand the production and transport mechanisms of ionospheric density structures because plasma enhancements affect the momentum and energy coupling between the ionosphere and thermosphere. Consequently, we conducted a systematic quantitative study of the origins, lifetimes, and transport characteristics of medium and large-scale density structures using our time-dependent, three-dimensional ionospheric model. We studied the formation of plasma 'blobs' or 'patches' due to particle precipitation in the dayside oval (papers 72 and 88), the effect that structured electric fields have on the ionosphere (paper 103), the extent to which large magnetic-field-aligned ion drifts affect density structures (paper 104), the effect of time-varying convection and precipitation patterns (papers 35 and 52), and the lifetimes and transport characteristics of density structures for different seasonal, solar cycle, and IMF conditions (papers 101 and 119).

The above studies were particularly useful for elucidating basic structuring processes. In particular, we found that: (1) Time-varying plasma convection and particle precipitation patterns can readily produce ionospheric structure on a variety of scales; (2) The observed electron precipitation in the polar cap can account for 'blob' creation if the plasma is exposed to the precipitation for 5–10 minutes; (3) Structured electric fields produce structured electron densities, ion temperatures, and ion composition; (4) The lifetime of an *F* region density structure depends on several factors, including the initial location where it was formed, the magnitude of the perturbation, season, solar cycle and IMF; and (5) Depending on the IMF, horizontal plasma convection can cause an initial structure to break up into multiple structures of various sizes, remain as a single distorted structure, or become stretched into elongated segments.

In order to model a convection pattern with electric field structure superimposed, measurements are needed not only along the satellite tract, but also in a direction perpendicular to the track, so that the entire spatial extent of the structure can be determined. Unfortunately, the required data set was not available and the model study (paper 103) had to be based on a semi-empirical description of electric field structure. The structure was assumed to be associated with a discrete current system into and out of the polar ionosphere; the current sheets for each structure were assumed to be sun-aligned and had a finite length. The potential disturbance associated with the structured current sheets was assumed to be a Volland two-cell pattern [*Volland*, 1978], as shown in Figure 5*a*. Each electric field structure was described by one such 2-cell pattern, but the spatial size of the structure and potential drop across it varied from structure to structure. In the model study, a total of 45 structures were randomly distributed in the polar cap.

The structured potential distribution was added to a standard, large-scale Volland potential distribution, which was used to simulate the background convection pattern. In the model study, eight representative convection trajectories were selected and flux tubes of plasma were followed as they convected along these trajectories across the polar cap in an anti-sunward direction. The calculations were done both with and without the electric field structure. The top panel of Figure 5*b* shows the trajectories for the unperturbed or background convection pattern, while the bottom panel shows the resulting trajectories when the structured electric fields are superimposed on the background pattern. The electric fields that would be measured by a satellite crossing these convection patterns along the dusk-dawn magnetic meridian are shown in Figure 5*c*. The top panel shows the electric field signature of a classical two-cell convection pattern, while the bottom panel shows the kind of structure that is frequently observed when the IMF is northward.

In the calculations, the trajectories were all started from daytime steady state conditions at the locations marked by the dot in Figure 5*b*, and the response of the plasma

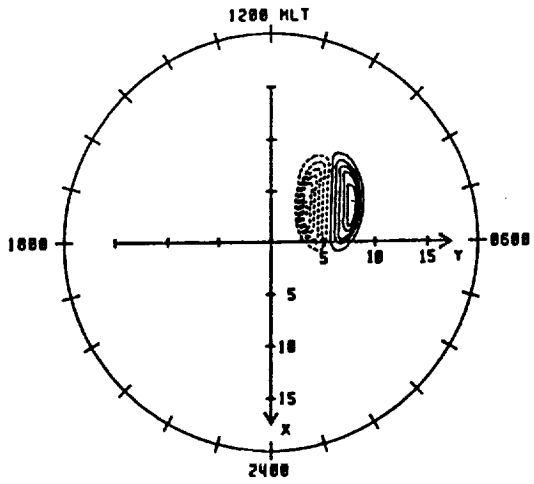

Figure 5*a*. Model of an electric field structure. Electric potential drawn at 1 kV intervals are shown in a magnetic x-y coordinate system. The potential varies from -6 to 6 kV for this structure.

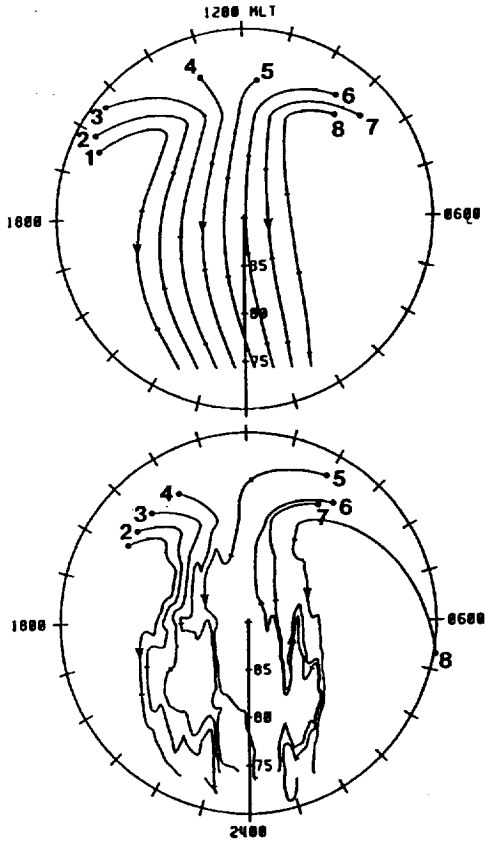

Figure 5*b*. Plasma trajectories for a 2-cell unperturbed convection pattern (top panel) and for a structured convection pattern (bottom panel) in the MLT-magnetic latitude reference frame. Circles denote the start location for each trajectory, while tick marks indicate one-hour time intervals.

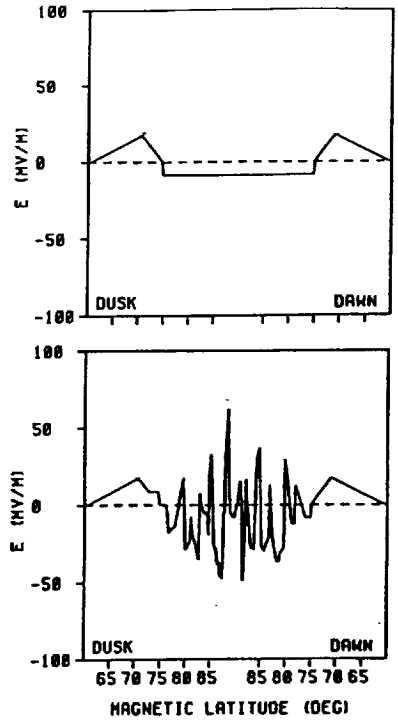

Figure 5*c*. Electric field variation along the dusk-dawn magnetic meridian for the unperturbed 2-cell convection pattern (top panel) and for the structured convection pattern (lower panel). The electric field is given in mV/m.

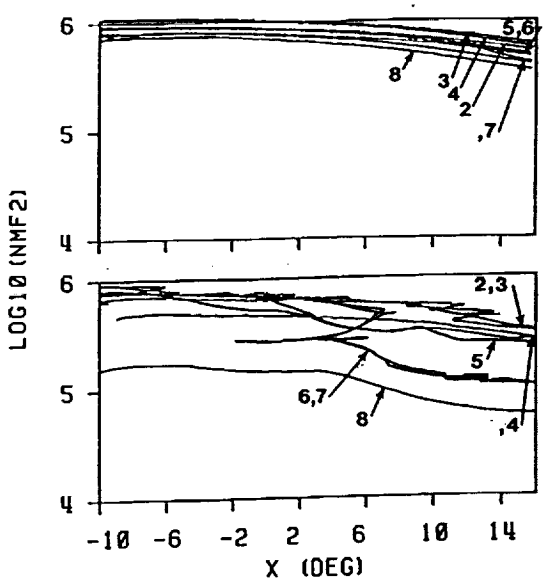

Figure 5*d*. $N_m F_2$ variation for each of the trajectories shown in Figure 5*b* plotted versus the flux tubes $\times$ location. The unperturbed (top) and perturbed (bottom) cases are shown. $\log_{10} N_m F_2 (\mathrm{cm}^{-3})$ is plotted. From Paper 103.

was calculated as the flux tubes followed their convection paths. Figure 5*d* shows how N_mF_2 varies along each trajectory for both the unperturbed (top panel) and structured (bottom panel) convection patterns. Note that the densities are plotted versus the trajectory x-axis (see Figure 5*a*). For the unperturbed pattern, the plasma following the eight trajectories convects across the polar cap and eventually into darkness, during which time N_mF_2 decays. However, the important feature to note is that the N_mF_2 variations for all eight trajectories are very similar. In sharp contrast, the N_mF_2 variations along the eight trajectories that contain structured electric fields are very different. Upon reaching the nightside auroral zone, the N_mF_2 values for the different flux tubes can differ by as much as an order of magnitude. The differences are a result of different transpolar crossing times and different 'localized' electric field strengths. Localized enhancements in the electric field produce ion temperature enhancements and increased $O^+ \rightarrow NO^+$ conversion rates [*Schunk et al.*, 1975], and this, in turn, yields lower N_mF_2 values.

Northward IMF Features

It is well known that the electric fields, particle precipitation, auroral conductivity enhancements, and Birkeland currents that couple the magnetosphere-ionosphere system are strongly dependent upon the direction of the IMF. When the IMF is southward, the Birkeland (or field-aligned) currents flow in the Region 1 and 2 current sheets, the *F* region plasma convection exhibits a two-cell structure with anti-sunward flow over the polar cap, the conductivity enhancements are confined to the statistical auroral oval, and the auroral electron precipitation is also confined to the classical oval. However, when the IMF is northward, the situation is considerably more complicated and less clear. In this case, an additional field-aligned current system occurs in the polar cap called the NBZ currents [*Maezawa*, 1976; *Iijima et al.*, 1984]; plasma convection can be sunward in the polar cap and the pattern can assume multi-cell, severely distorted two-cell or turbulent characteristics [*Burke et al.*, 1979; *Potemra et al.*, 1984; *Frank et al.*, 1986; *Heppner and Maynard*, 1987]; and particle precipitation occurs in the polar cap which can be uniform, in the form of multiple sun-aligned arcs, or in a θ-aurora configuration [*Buchau et al.*, 1983; *Frank et al.*, 1986].

We conducted a number of theoretical studies in an effort to elucidate the ionospheric conditions for northward IMF. Using an *E* region conductivity model we developed (paper 111) and our polar electrodynamic model, we conducted the *first* current-conductivity simulations for northward IMF. In our first paper, we considered the magnetosphere to be both a 'constant current source' and a 'constant voltage source' and determined the conditions leading to *idealized* two-cell, three-cell, and four-cell plasma convection patterns (paper 95). When the various cases were compared with measurements, our results indicated that the magnetosphere acts more like a voltage source than a current source.

Subsequently, *Iijima and Shibaji* [1987] presented empirical models of Birkeland currents for different IMF B_y and B_z conditions, and we used these current patterns in our electrodynamic simulations in an effort to determine whether three-cell, four-cell, or distorted two-cell convection patterns occur for northward B_z (paper 116). Unfortunately, because of a data gap on the dayside at latitudes equatorward of about 80° magnetic, the measured NBZ currents had to be extrapolated in the noon sector. Depending on how the currents were extrapolated, different convection patterns could be obtained. Figure 6 illustrates the above problem for the case when the IMF is strongly northward ($B_z > B_y > 0$). Shown in the upper-left dial of this figure are the unmodified Birkeland currents measured by *Iijima and Shibaji* [1987]. The upper-right dial, on the other hand, shows a possible extension of these currents into the dayside where measurements are lacking. The

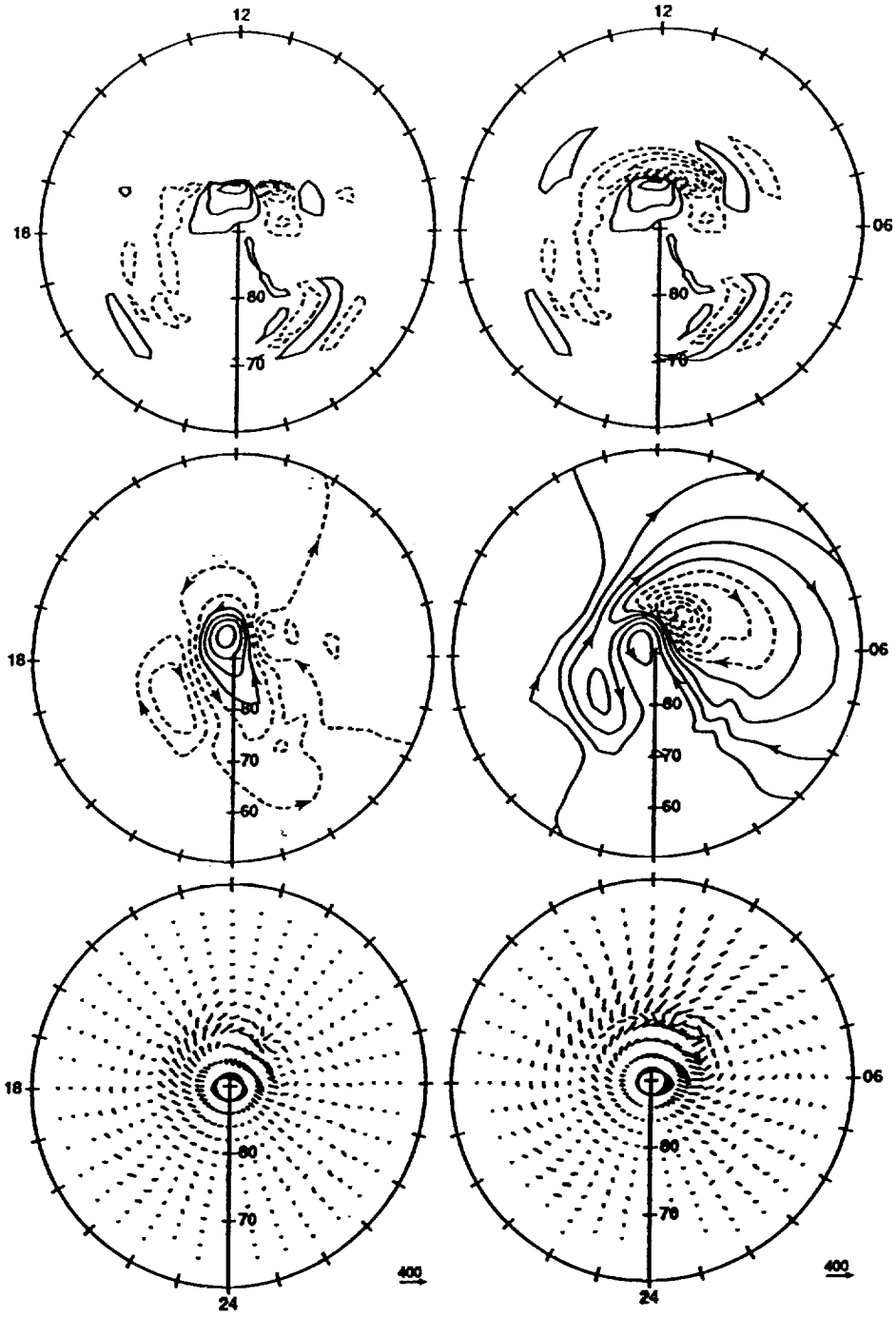

Figure 6. Birkeland currents (upper panel), ionospheric electric potential (middle panel) and ionospheric currents (lower panel) for $B_z > B_y > 0$. The upper-left dial represents the unmodified Birkeland currents of *Iijima and Shibaji* [1987], while the currents in the upper-right dial have been extended into the dayside and nightside. In the upper panel, current flowing into the ionosphere is plotted as solid curves, while current flowing away from the ionosphere is plotted as dashed curves (the difference between contour levels is 0.3 $\mu A/m^2$). In the middle panel the difference between contour levels is 3 kV. For the lower panel the vector scale is 400 A/km. From Paper 116.

extension was accomplished by interpolating along lines of constant latitude so that the dusk Region 1 system connects to the dawnside NBZ system. The electric potential patterns calculated from the two Birkeland current patterns are shown in the middle panel. In comparing the two potential patterns, it is apparent that the extension of the current on the dayside is important for northward IMF. For the unmodified currents on the left-hand side, the flow in the morning sector is broken into multiple cells. Although there is evidence for three-cell convection, the NBZ currents are so strong in comparison to the net Region 1/Region 2 currents, that the strongest flow occurs within the polar cap and the rotation of the equatorward cell in the dawn sector is reversed from its normal sense. For the dayside extension of the currents in the upper-right dial, the flow also has a three-cell nature, but because of the connection of flow on the dayside, convection appears more as a distorted two-cell pattern similar to that shown by *Heppner and Maynard* [1987]. Although the convection pattern described above supports the distorted two-cell configuration suggested by *Heppner and Maynard* [1987], different extrapolations of the NBZ current system in the noon sector can produce both three-cell and four-cell convection patterns.

Once the convection patterns for northward IMF are identified, we have the additional capability of determining their effect on the *F* region. For example, in one study the *idealized* multi-cell plasma convection patterns described above for northward IMF were used in conjunction with our time-dependent, three-dimensional ionospheric model in order to study the characteristic *F* region signature associated with multi-cell convection patterns (paper 86). As expected, there are major distinguishing *F* region features associated with the different convection patterns, particularly in the polar cap in *winter* (Figure 7). For two-cell convection, the anti-sunward flow of plasma from the dayside into the polar cap acts to maintain the densities in this region. For four-cell convection, on the other hand, the two additional convection cells in the polar cap are in darkness most of the time, and the resulting O^+ density decay acts to produce twin polar holes that are separated by a sun-aligned ridge of enhanced ionization due to θ-aurora precipitation. For three-cell convection, only one polar hole forms (not shown).

Stability of Macroscopic Flows

Numerous mathematical formulations have been used over the years to describe plasma flows in the solar-terrestrial environment, including magnetohydrodynamic, kinetic, semi-kinetic, hydromagnetic, generalized moment, and hydrodynamic formulations. All of these formulations have intrinsic limitations when applied to three-dimensional macroscopic flows. For example, the kinetic and semi-kinetic formulations are usually applied to steady state situations, and hence, wave phenomena are not included. Also, although time-dependent MHD and hydrodynamic models allow for wave excitation, only low frequency waves are possible. Hence, in general, the microphysics (non-Maxwellian distributions, plasma instabilities, wave-particle interactions, etc.) is not included in full-scale global simulations.

Unstable flow conditions can occur in a variety of situations. For example, the edges of convecting *F* region blobs and patches are susceptible to gradient-drift instabilities [cf. *Tsunoda,* 1988], but these instabilities generally don't affect the large-scale flow. Also, in regions of rapid $\mathbf{E} \times \mathbf{B}$ convection, the ion velocity distributions in the *E* and *F* regions can become highly non-Maxwellian [cf. *St.-Maurice and Schunk*, 1979; *Hubert*, 1983; *Lockwood et al.*, 1987] and the resulting instabilities could affect ionosphere-thermosphere momentum and energy coupling. Likewise, the large-scale horizontal currents that flow in the *E* region (see Figure 4) are susceptible to Farley-Buneman instabilities [cf. *St.-Maurice*, 1985; *Haldoupis*, 1989]. Finally, we note that the polar wind distributions predicted by the macroscopic models are highly non-Maxwellian and

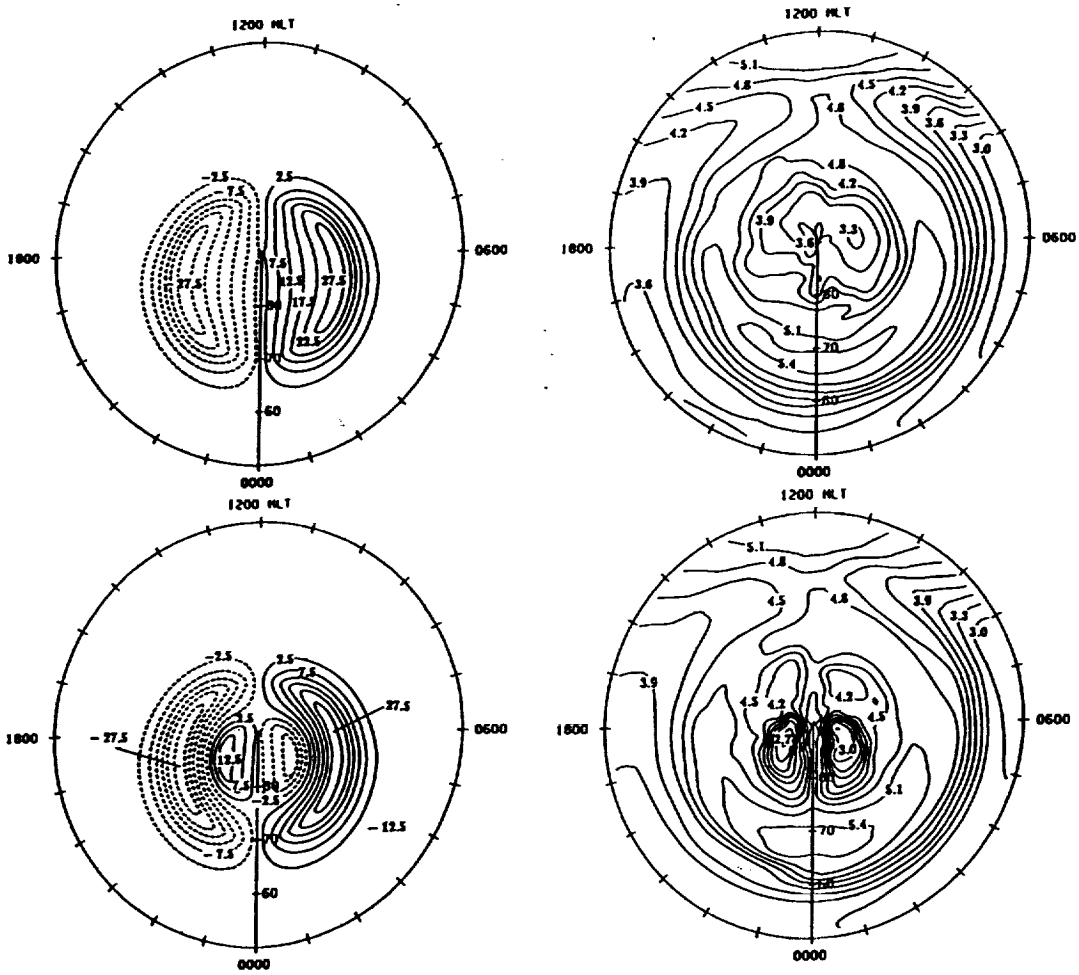

Figure 7. Contours of electrostatic potential (left panel) and $\log_{10}$ O^+ density (right panel) at 300 km for both two-cell (top row) and four-cell (bottom row) plasma convection patterns. An MLT-magnetic latitude coordinate system is used. From Paper 86.

potentially unstable, particularly when energetic beams and conics pass through the polar wind. Therefore, when macroscopic models are used to predict plasma flow conditions, it is important to study the stability of the predicted flows. Part of our NASA Theory Program was devoted to such an effort and in the following paragraphs we highlight our polar wind instability studies.

The classical polar wind corresponds to an outflow of thermal plasma from the high latitude ionosphere. Above about 3000 km, the H^+ flow becomes supersonic and collisionless, and the H^+ velocity distribution function becomes highly non-Maxwellian. The non-Maxwellian features include a temperature anisotropy with $T_i^{\parallel} > T_i^{\perp}$ and an asymmetry in the form of an elongated tail in the upward direction. At a distance of 10 earth radii, $T_i^{\parallel} / T_i^{\perp} \sim 50$. Since this highly non-Maxwellian H^+ velocity distribution is potentially unstable and since the resulting wave-particle interactions could have a significant effect on the flow of mass, momentum, and energy between the polar ionosphere and magnetosphere, we studied the linear stability of the polar wind with regard to the excitation of electrostatic waves (paper 93). Despite the highly non-Maxwellian character of the H^+ distribution function, we found that the 'classical' polar wind is remarkably stable for a wide range of conditions.

Although the classical polar wind occurs the bulk of the time, during increasing magnetic activity and for certain flux tubes that pass through the cusp, the classical picture of the polar wind may not be appropriate. Figure 8 shows schematically a possible mechanism by which the polar wind deviates from the classical picture due to plasma convection. As the flux tube convects into the cusp region, the ions at low altitudes undergo parallel and perpendicular energization. These energetic ions eventually catch up with the slower "classical" polar wind at high altitudes as the flux tube convects into the polar cap region. The stability of a cusp-generated H^+ beam passing through the classical polar wind was studied in paper 123. The stability of the plasma was studied for a range of electron-ion temperature ratios ($0.1 \leq T_e/T_i \leq 10$) and beam-to-background ion density ratios ($0.1 \leq n_b/(n_b + n_i) \leq 0.9$). Table 1 summarizes the results found in our study. For most of the cases, the polar wind is unstable for fairly small ion beam-plasma relative drifts. The plasma is more unstable for larger electron temperatures and for comparable ion beam and background ion densities ($n_b \sim n_i$). For large electron temperatures ($T_e = 10\ T_i$), the ion/ion plasma-acoustic instability is the first mode to be triggered, and the waves that propagate parallel to the magnetic field are destabilized first. For lower electron temperatures, the ion/ion cyclotron modes tend to be triggered first.

Auroral Dynamics

We used our 2.5-dimensional particle-in-cell (PIC) code to study auroral plasma processes (papers 90 and 91). In particular, we conducted a systematic study of the plasma processes driven by a field-aligned current sheet with a finite thickness perpendicular to the **B** field. Both wide and narrow (relative to the ion gyroradius) current sheets were considered. In these simulations, we observed double layers, upflowing ions in the form of beams and conics, both upflowing and downflowing accelerated electron beams, several wave modes (EIC, lower hybrid, VLF, ELF, and HF), and associated nonlinear plasma phenomena.

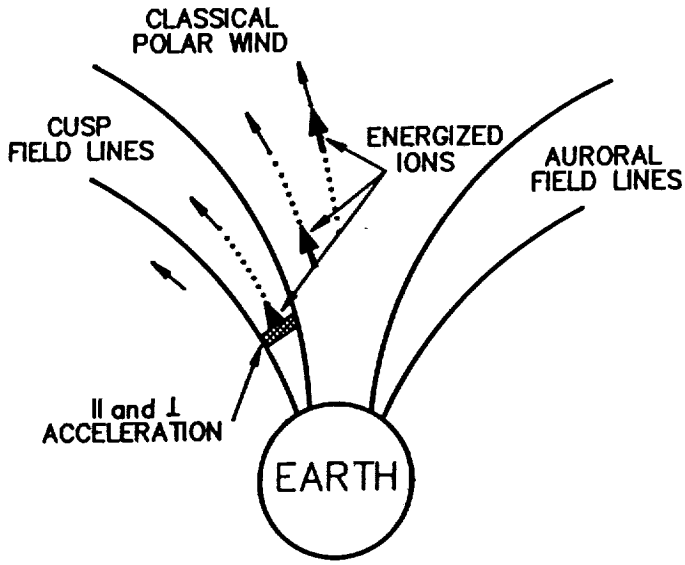

Figure 8. Schematic diagram showing how ion acceleration in the cusp coupled with horizontal plasma convection can lead to an energetic ion population passing through the classical polar wind. From Paper 123.

Table 1. H^+ beam-plasma normalized critical drift velocity above which the plasma is unstable for different electron-to-ion temperature ratios and different beam-to-background ion density ratios for $T_b/T_i = 0.1$. The critical drift velocity is normalized with respect to the parallel thermal speed of the background ions. From Paper 123.

T_e/T_i	$n_b/(n_b + n_i)$		
	0.1	0.5	0.9
0.1	> 11	3.4	> 11
1.0	2.7	0.71	1.30
10	0.3	0.18	0.26

Subsequently, our attention was focused on studying the effect that auroral processes have on the ionospheric densities and temperatures. In paper 97, we studied the effect of ionospheric return currents on auroral electron temperatures. This study was motivated by the fact that in a partially-ionized plasma an electron heat flow can occur in response to either an electron temperature gradient (thermal conduction) or an electron current (thermoelectric heat flow). The former process has been extensively studied, while the latter process has received relatively little attention. Therefore, we used our time-dependent, three-dimensional model of the high-latitude ionosphere to study the effect of field-aligned ionospheric return currents on auroral electron temperatures for different seasonal and solar cycle conditions as well as for different heat fluxes at our upper boundary (800 km).

Figure 9 shows electron temperature profiles for three values of the field-aligned return current for summer and winter conditions at solar minimum. The field-aligned currents are 0 (solid curves), -1×10^{-5} (dotted curves), and -5×10^{-5} (dashed curves) amp m^{-2}. The profiles were calculated with the total heat flow through the upper boundary set to zero. The solid curves correspond to the typical case of no field-aligned current and no heat flow through the upper boundary. Consequently, the electron temperature is constant at high altitudes owing to the dominance of thermal conduction. For all cases shown in Figure 9, thermoelectric heat transport corresponds to an upward flow of energy at all altitudes, but it can be a source or sink of heat depending on the shape of the electron density profile. For example, if we consider the solar minimum-winter case with $J_{\|} = -5 \times 10^{-5}$ amp m^{-2}, thermoelectric heat transport is a sink below 200 km, a source between 200 and 280 km, and a sink above 280 km. The effect of an increased magnitude of the return current is merely to enhance this result.

Plasma Expansion Phenomena

We also studied plasma expansion phenomena. Based on the pioneering work of *Gurevich et al.* [1966] and subsequent work [cf. *Samir et al.*, 1983], it is now well known that during a rapid plasma expansion, the ion distribution functions can depart significantly from a Maxwellian, and consequently, superthermal tails, plasma instabilities and wave-particle interactions may be important. From the macroscopic modelling viewpoint, it is important to understand the basic physics involved in a plasma expansion so that reliable macroscopic models can be developed for a range of solar-terrestrial applications (solar wind, polar wind, interhemispheric flow, etc.).

Our work in this area involved both *small-scale* and *macroscopic* plasma expansions. Initially, we obtained a numerical solution of the time-dependent Vlasov-Poisson system and studied single-ion (H^+), multi-ion (H^+, O^+), and counterstreaming (H^+ -H^+) plasma expansions (papers 26, 33, and 42). These *small-scale* simulations were for *collisionless, one-dimensional* plasmas, and hence, were relevant to plasma expansions along a magnetic field. However, since the **B** field was not included in these simulations, the excitation of certain wave modes (EIC, lower hybrid, etc.) was excluded. Consequently, we then conducted 2.5-dimensional PIC simulations for *collisionless* plasma expansions *along* a **B** field so that the results could be compared to the 1-D cases (paper 79). We also conducted *macroscopic* (hydrodynamic) plasma expansions to model conditions in the *collisionless* polar wind (papers 68, 81, and 115). Again, these studies were for expansions *along* the **B** field. We found that many of the expansion characteristics seen in the small-scale simulations were also seen in the macroscopic simulations, but the macroscopic simulations produced additional results not contained in the small-scale simulations and vice versa.

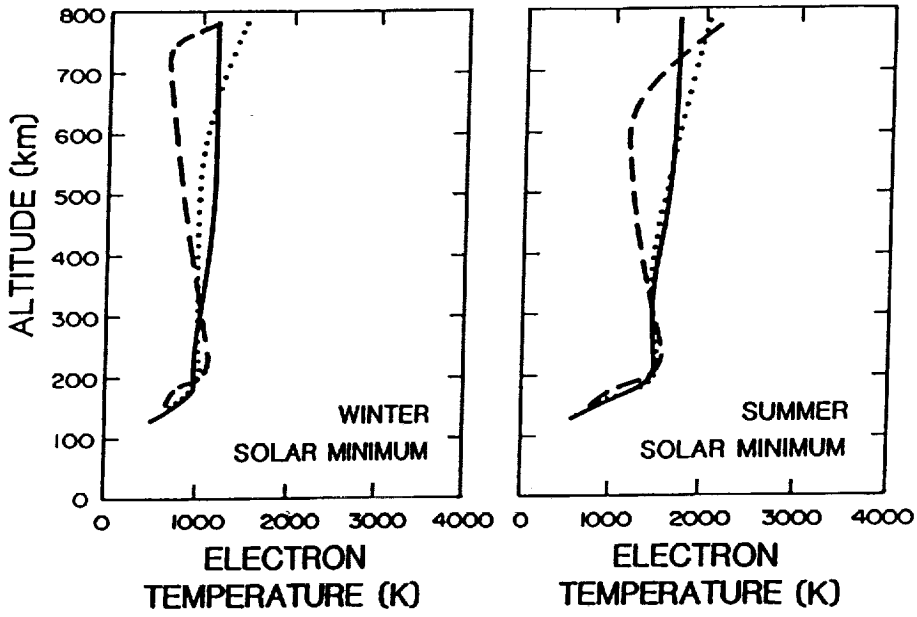

Figure 9. Electron temperature profiles in the nocturnal auroral oval for three values of the field-aligned return current at solar minimum for both summer and winter conditions. The field-aligned current values are 0 (solid curves), -1×5^{-5} (dotted curves), and -5×10^{-5} (dashed curves) amp m^{-2}. From Paper 97.

Our most recent work involved *macroscopic* plasma expansions *across* a magnetic field including the effect of collisions (paper 134). The model we developed is based on a numerical solution of the time-dependent, nonlinear, coupled continuity and momentum equations for the expanding ions, background ions, and electrons. In this model, the equations are height-integrated so that only plasma expansions across the geomagnetic field can be modelled (i.e., 2-D model). In a model simulation, a neutral gas or plasma is injected into the ionosphere and the subsequent temporal evolution is followed. The model takes into account ionization processes, chemical reactions, pressure gradients, ion inertia, stress tensor (collisional viscosity and finite Larmor radius effect), gravity, Coulomb collisions between the different charged particles, ion collisions with both the background and injected neutrals, and polarization electric fields in both the expanding and background plasmas. Figure 10 shows an example of the 2-D simulation results. This figure compares the expansion characteristics for gases released at 200 and 400 km. The two cases are for similar conditions; 10 kilogram Barium release with an initial cloud radius of 2 km and a release velocity of 5 km/s perpendicular to **B**, which is directed out of the figure. Shown in Figure 10 are contours of the ion cloud Pedersen conductivity and the ion velocity field at $t = 1$, 10, and 25 seconds after the gas release. Also shown in the figure is the motion of the neutral *Ba* cloud, which can be clearly seen at 400 km. The neutral cloud is shown by a single circle that expands as it moves in the released gas direction (upward in the figure). In comparing similar *Ba* releases at 400 and 200 km, the following features are evident: (1) at both altitudes, the ion clouds skid across magnetic field lines; (2) the expansion of both the ion and neutral clouds is slower at low altitudes than at high altitudes; (3) the cloud Pedersen conductivity is about 200 times greater at 200 km than at 400 km; and (4) the ion cloud expansion is more symmetric at 200 km than at 400 km.

Solar Wind/Interplanetary Medium

Recently, we used generalized transport equations for both *subsonic* flow along SAR-arc field lines (paper 94) and for the *supersonic* polar wind (papers 98 and 120). These bi-Maxwellian-based 16-moment transport equations have an advantage over both the standard collision-dominated transport equation (Chapman and Enskog equations) and the collisionless kinetic equations in that they can describe both collision-dominated and collisionless regimes and provide a continuous transition between them. In the collision-dominated regime, they reduce to the usual diffusion and thermal conduction equations, while in the collisionless regime they describe temperature anisotropies and collisionless heat flow to the same level as kinetic equations. Another advantage is that velocity distribution functions can be readily obtained at any point in space. As a spinoff of this work, we applied the equations to the *solar wind* and were able to obtain solutions from 30 R_S (solar radii) to the orbit of the Earth at 215 R_S (papers 131 and 135). We found that the bi-Maxwellian based 16-moment equations can properly describe the evolution of the proton distribution function [*Marsch et al.*, 1982].

In order to achieve our ultimate goal of obtaining a numerical model of the solar-terrestrial system from the solar corona to the lower thermosphere, we developed both 2-D and 3-D hydrodynamic models and a 2-D MHD model of steady corotating solar wind streams (papers 117 and 118). All three models were used to study the latitudinal structure of the solar wind. We found that with the MHD model the latitudinal structure of the steady solar wind is decided by a dynamic balance between the magnetic and gas pressures. Our calculations also indicated the existence of a proton number density maximum around the magnetic neutral line regardless of whether there was a density maximum or minimum at our inner boundary at 0.15 AU.

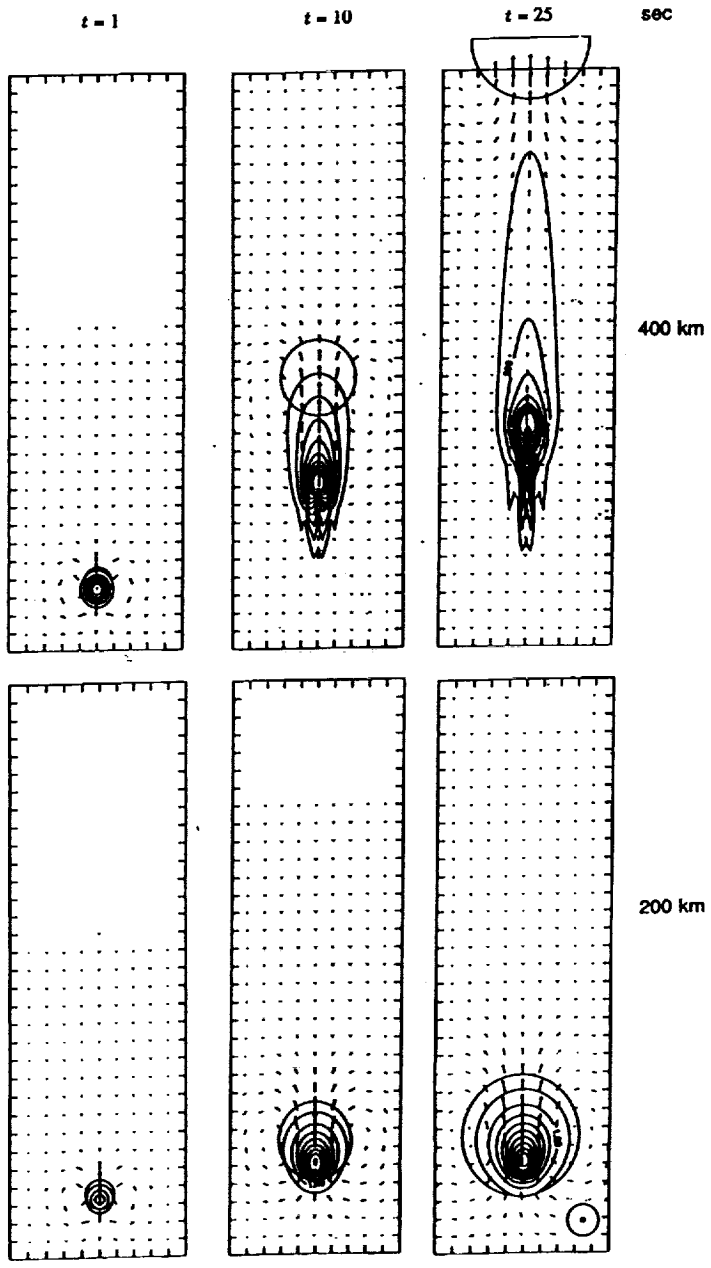

Figure 10. Contours of the ion cloud Pedersen conductivity and the ion velocity field at $t = 1$, 10, and 25 seconds after Barium releases at 400 km (top panel) and 200 km (bottom panel). The B field is directed out of the figure. The contour separation is 10^{-3} mho in the upper panel and 0.5 mho in the lower panel. From Paper 134.

REFERENCES

Ahn, B.-H., Y. Kamide, and S.-I. Akasofu, *J. Geophys. Res., 91,* 5737, 1986.

Brice, N. M., *J. Geophys. Res., 72,* 5193, 1967.

Buchau, J., B. W. Reinisch, E. J. Weber, and J. G. Moore, *Radio Sci., 18,* 995, 1983.

Buchau, J., et al., *Radio Sci., 20,* 325, 1985.

Burke, W. J., M. C. Kelley, R. C. Sagalyn, M. Smiddy, and S. T. Lai, *Geophys. Res. Lett., 6,* 21, 1979.

de la Beaujardiere, O., et al., *J. Geophys. Res., 90,* 4319, 1985.

Frank, L. A., et al., *J. Geophys. Res., 91,* 3177, 1986.

Fuller-Rowell, T. J., and D. Rees, *Planet. Space Sci., 31,* 1209, 1983.

Gurevich, A. V., L. V. Pariiskaya, and L. P. Pitaevskii, *Sov. Phys. JETP Eng. Transl., 22,* 449, 1966.

Haldoupis, C., *AGARD Conf. Proc., 441,* Paper 31, 1989.

Heelis, R. A., P. H. Reiff, J. D. Winningham, and W. B. Hanson, *J. Geophys.. Res., 91,* 5817, 1986.

Heppner, J. P., and N. Maynard, *J. Geophys. Res., 92,* 4467, 1987.

Horwitz, J. L., *J. Atmos. Terr. Phys., 45,* 765, 1983.

Hubert, D., *Planet. Space Sci., 31,* 119, 1983.

Iijima, T., and T. Shibaji, *J. Geophys. Res., 92,* 2408, 1987.

Iijima, T., T. A. Potemra, L. J. Zanetti, and P. F. Bythrow, *J. Geophys. Res., 89,* 7441, 1984.

Intriligator, D. S., *Nat. Res. Counc.,* National Academy Press, Washington, D.C., 1984.

Kamide, Y., J. D. Craven, L. A. Frank, B.-H. Ahn, and S.-I. Akasofu, *J. Geophys. Res., 91,* 11,235, 1986.

Kelley, M. C., J. F. Vickrey, C. W. Carlson, and R. Torbert, *J. Geophys. Res., 87,* 4469, 1982.

Lee, M. C., *J. Geophys. Res., 89,* 2289, 1984.

Lemaire, J., *Frontiers of the Plasmasphere,* Universite Catholique de Louvain, Cabay, Louvain-la-Neuve, Belgium, 1985.

Liu, C. H., and B. Edwards, World-wide ionosphere-thermosphere study, *WITS Handbook, Vol. 1,* University of Illinois, 1988.

Lockwood, M. et al., *Geophys. Res. Lett., 14,* 111, 1987.

Maezawa, K., *J. Geophys. Res., 81,* 2289, 1976.

Marsch, E., et al., *J. Geophys. Res., 87,* 52, 1982.

Nishida, A., *J. Geophys. Res., 71,* 5669, 1966.

Potemra, T. A., et al., *J. Geophys. Res., 89,* 9753, 1984.

Richmond, A. D., and Y. Kamide, *J. Geophys. Res., 93,* 5741–5759, 1988.

Robinson, R. M., et al., *J. Geophys. Res., 90,* 7533, 1985.

Roble, R. G., E. C. Ridley, A. D. Richmond, and R. E. Dickinson, *Geophys. Res. Lett., 15,* 1325, 1988.

Roederer, J. G., *EOS, 69,* 786, 1988.

Romick, G. J., T. L. Killeen, D. G. Torr, B. A. Tinsley, and R. A. Behnke, CEDAR Program, *EOS, 68,* 19, 1987.

St.-Maurice, J.-P., *J. Geophys. Res., 90,* 5211, 1985.

St.-Maurice, J.-P., and R. W. Schunk, *Rev. Geophys. & Space Phys., 17,* 99, 1979.

Samir, U., K. H. Wright, and H. H. Stone, *Rev. Geophys. & Space Phys., 21,* 1631, 1983.

Schunk, R. W., Magnetosphere-ionosphere-thermosphere coupling processes, *WITS Handbook,* 1989.
Schunk, R. W., W. J. Raitt, and P. M. Banks, *J. Geophys. Res., 80,* 3121, 1975.
Tsunoda, R. T., *Rev. Geophys., 26,* 719, 1988.
Volland, H. *J. Geophys. Res., 83,* 2695, 1978.
Weber, E. J., et al., *J. Geophys. Res., 89,* 1683, 1984.
Weber, E. J., et al., *J. Geophys. Res., 91,* 12,121, 1986.

Cumulative STTP Publications

1. W. J. Raitt, R. W. Schunk, and J. J. Sojka, Modelling the high-latitude ionosphere, Proceedings of the AGARD/NATO Symposium on *The Physical Basis of the Ionosphere in the Solar-Terrestrial System,* 9.1–9.14, Pozzuoli, Italy, 1980.

2. R. W. Schunk and D. S. Watkins, Electron temperature anisotropy in the polar wind, *J. Geophys. Res., 86,* 91–102, 1981.

3. P. M. Banks, W. F. Edwards, C. Rasmussen, and R. C. Thompson, Applications of the concept of generalized vorticity to space plasmas, *Geophys. Res. Lett., 8,* 95–98, 1981.

4. J. J. Sojka, W. J. Raitt, and R. W. Schunk, A theoretical study of the high-latitude winter *F* region at solar minimum for low magnetic activity, *J. Geophys. Res., 86,* 609–621, 1981.

5. J. J. Sojka, W. J. Raitt, and R. W. Schunk, Theoretical predictions for ion composition in the high-latitude winter *F*-region for solar minimum and low magnetic activity, *J. Geophys. Res., 86,* 2206–2216, 1981.

6. A. R. Barakat and R. W. Schunk, Momentum and energy exchange collision terms for interpenetrating bi-Maxwellian gases, *J. Phys. D: Appl. Phys., 14,* 421–438, 1981.

7. R. W. Schunk, W. J. Raitt, and J. J. Sojka, High-latitude ionospheric model: First step towards a predictive capability, Proceedings of the Symposium on *Effect of the Ionosphere on Radiowave Systems,* 599–609, Alexandria, Virginia, 1981.

8. R. W. Schunk and J.-P. St.-Maurice, Ion temperature anisotropy and heat flow in the Venus lower ionosphere, *J. Geophys. Res., 86,* 4823–4827, 1981.

9. P. G. Richards and D. G. Torr, A formula for calculating theoretical photoelectron fluxes resulting from the He^+ 304 Å solar spectral line, *Geophys. Res. Lett., 8,* 995–998, 1981.

10. J. J. Sojka, W. J. Raitt, and R. W. Schunk, Plasma density features associated with strong convection in the winter high-latitude *F* region, *J. Geophys. Res., 86,* 6908–6916, 1981.

11. J.-P. St.-Maurice and R. W. Schunk, Ion-neutral momentum coupling near discrete high-latitude ionospheric features, *J. Geophys. Res., 86,* 11,299–11,321, 1981.

12. N. Singh, R. W. Schunk, and J. J. Sojka, Energization of ionospheric ions by electrostatic hydrogen cyclotron waves, *Geophys. Res. Lett., 8*, 1249–1252, 1981.

13. A. R. Barakat and R. W. Schunk, Transport equations for multicomponent anistropic space plasmas: A review, *Plasma Phys., 24*, 389–418, 1982.

14. N. Singh, Double layer formation, *Plasma Phys., 24*, 639–660, 1982.

15. J. J. Sojka, W. J. Raitt, R. W. Schunk, F. J. Rich, and R. C. Sagalyn, Observations of the diurnal dependence of the high-latitude *F* region ion density by DMSP satellites, *J. Geophys. Res., 87*, 1711–1718, 1982.

16. N. Singh and R. W. Schunk, Dynamical features of moving double layers, *J. Geophys. Res., 87*, 3561–3580, 1982.

17. R. W. Schunk and D. S. Watkins, Proton temperature anisotropy in the polar wind, *J. Geophys. Res., 87*, 171–180, 1982.

18. J. J. Sojka, R. W. Schunk, and W. J. Raitt, Seasonal variations of the high-latitude *F* region for strong convection, *J. Geophys. Res., 87*, 187–198, 1982.

19. A. R. Barakat and R. W. Schunk, Comparison of transport equations based on Maxwellian and bi-Maxwellian distributions for anisotropic plasmas, *J. Phys. D: Appl. Phys., 15*, 1195–1216, 1982.

20. J. J. Sojka and R. W. Schunk, Predicted diurnal variations of electron density for three high-latitude incoherent scatter radars, *Geophys. Res. Lett., 9*, 143–146, 1982.

21. R. W. Schunk and J. J. Sojka, Ion temperature variations in the daytime high-latitude *F* region, *J. Geophys. Res., 87*, 5169–5183, 1982.

22. P. G. Richards, D. G. Torr, and P. J. Espy, Determination of photoionization branching ratios and total photoionization cross sections of 304 Å from experimental ionospheric photoelectron fluxes, *J. Geophys. Res., 87*, 3599–3611, 1982.

23. N. Singh and R. W. Schunk, Current carrying properties of double layers and low frequency auroral fluctuations, *Geophys. Res. Lett., 9*, 446–449, 1982.

24. A. R. Barakat and R. W. Schunk, Comparison of Maxwellian and bi-Maxwellian expansions with Monte Carlo simulations for anisotropic plasmas, *J. Phys. D: Appl. Phys., 15*, 2189–2203, 1982.

25. P. G. Richards, M. R. Torr, and D. G. Torr, The seasonal effect of nitric oxide cooling on the thermospheric U.V. heat budget, *Planet. Space Sci., 30*, 515–518, 1982.

26. N. Singh and R. W. Schunk, Numerical calculations relevant to the initial expansion of the polar wind, *J. Geophys. Res., 87*, 9154–9170, 1982.

27. R. W. Schunk and J. J. Sojka, Ionospheric hot spot at high latitudes, *Geophys. Res. Lett., 9*, 1045–1048, 1982.

28. N. Singh, R. W. Schunk, and J. J. Sojka, Cyclotron resonance effects on stochastic acceleration of light ionospheric ions, *Geophys. Res. Lett., 9,* 1053–1056, 1982.

29. N. Singh and R. W. Schunk, Current-driven double layers and the auroral plasma, *Geophys. Res. Lett., 9*, 1345–1348, 1982.

30. J. J. Sojka, J. C. Foster, P. M. Banks, and J. R. Doupnik, Mapping electrostatic potentials from the ionosphere to the magnetosphere, *Planet. Space Sci., 31*, 1329–1338, 1983.

31. P. G. Richards and D. G. Torr, A simple theoretical model for calculating and parameterizing the ionospheric photoelectron flux, *J. Geophys. Res., 88*, 2155–2162, 1983.

32. W. J. Raitt and R. W. Schunk, Composition and characteristics of the polar wind, In, "Energetic Ion Composition in the Earth's Magnetosphere," Editor, R. G. Johnson, 99–141, 1983.

33. N. Singh and R. W. Schunk, Expansion of a multi-ion plasma into a vacuum, *Phys. Fluids, 26*, 1123–1128, 1983.

34. N. Singh, R. W. Schunk, and J. J. Sojka, Preferential perpendicular acceleration of heavy ionospheric ions by interactions with electrostatic hydrogen cyclotron waves, *J. Geophys. Res., 88*, 4055–4066, 1983.

35. J. J. Sojka and R. W. Schunk, A theoretical study of the high latitude *F* region's response to magnetospheric storm inputs, *J. Geophys. Res., 88,* 2112–2122, 1983.

36. R. W. Schunk, The terrestrial ionosphere, Proceedings of the "Theory Institute in Solar-Terrestrial Physics," Editors, R. L. Carovillano and J. M. Forbes, 609–676, 1983.

37. A. R. Barakat, R. W. Schunk, and J.-P. St.-Maurice, Monte Carlo calculations of the O^+ velocity distribution in the auroral ionosphere, *J. Geophys. Res., 88*, 3237–3241, 1983.

38. H. Thiemann, N. Singh, and R. W. Schunk, Formation of V-shaped potentials, Sixth ESA Symposium on European Rocket and Balloon Programs, *ESA SP–183*, 269–275, 1983.

39. P. G. Richards, R. W. Schunk, and J. J. Sojka, Large-scale counterstreaming of H^+ and He^+ along plasmaspheric flux tubes, *J. Geophys. Res., 88*, 7879–7886, 1983.

40. H. Thiemann and N. Singh, Further observations on resonance cones in non-Maxwellian plasmas, *Radio Sci., 18*, 615–624, 1983.

41. J. J. Sojka, R. W. Schunk, J. V. Evans, J. M. Holt, and R. H. Wand, Comparison of model high-latitude electron densities with Millstone Hill observations, *J. Geophys. Res., 88*, 7783–7793, 1983.

42. N. Singh and R. W. Schunk, Numerical simulations of counterstreaming plasmas and their relevance to interhemispheric flows, *J. Geophys. Res., 88*, 7867–7877, 1983.

43. N. Singh and R. W. Schunk, Comparison of the characteristics of potential drop and current-driven double layers, *J. Geophys. Res., 88*, 10,081–10,090, 1983.

44. W. Li, J. J. Sojka, and W. J. Raitt, A study of plasmaspheric density distributions for diffusive equilibrium conditions, *Planet. Space Sci., 31*, 1315–1327, 1983.

45. J. J. Sojka, R. W. Schunk, J. F. E. Johnson, J. H. Waite, and C. R. Chappell, Characteristics of thermal and suprathermal ions associated with the dayside plasma trough as measured by the Dynamics Explorer retarding ion mass spectrometer, *J. Geophys. Res., 88*, 7895–7911, 1983.

46. N. Singh, H. Thiemann, and R. W. Schunk, Simulation of auroral current sheet equilibria and associated V-shaped potential structures, *Geophys. Res. Lett., 10*, 745–748, 1983.

47. A. R. Barakat and R. W. Schunk, O^+ ions in the polar wind, *J. Geophys. Res., 88*, 7887–7894, 1983.

48. N. Singh and R. W. Schunk, Collisionless electron shocks in electron-beam-plasma systems, *Phys. Fluids, 26*, 2781–2783, 1983.

49. J. Murdin, J. J. Sojka, and R. W. Schunk, Diurnal transport effects on the *F*-region plasma at Chatanika under quiet and disturbed conditions, *Planet. Space Sci., 32*, 47–61, 1984.

50. N. Singh, R. W. Schunk, and J. R. Conrad, Electrostatic hydrogen-cyclotron wave emission below the hydrogen-cyclotron frequency in the auroral acceleration region, *J. Geophys. Res., 89,* 1650–1654, 1984.

51. N. Singh and R. W. Schunk, Energization of ions in the auroral plasma by broadband waves: Generation of ion conics, *J. Geophys. Res., 89,* 5538–5546, 1984.

52. J. J. Sojka and R. W. Schunk, A theoretical *F* region study of ion compositional and temperature variations in response to magnetospheric storm inputs, *J. Geophys. Res., 89,* 2348–2358, 1984.

53. N. Singh and R. W. Schunk, Plasma response to the injection of an electron beam, *Plasma Phys., 26,* 859–890, 1984.

54. A. R. Barakat and R. W. Schunk, Effect of hot electrons on the polar wind, *J. Geophys. Res., 89,* 9771–9783, 1984.

55. A. R. Barakat and R. W. Schunk, O^+ charge exchange in the polar wind, *J. Geophys. Res., 89,* 9835–9839, 1984.

56. N. Singh and R. W. Schunk, The relationship between the electric fields associated with plasma expansion and double layers, Proceedings of the *Second Symposium on Plasma Double Layers and Related Topics,* 272–277, 1984.

57. N. Singh and R. W. Schunk, Can Buneman double layers be driven in auroral plasmas?, Proceedings of the *Second Symposium on Plasma Double Layers and Related Topics,* 364–369, 1984.

58. N. Singh, H. Thiemann, and R. W. Schunk, Current fluctuations and dynamical features of double layer potential profiles, Proceedings of the *Second Symposium on Plasma Double Layers and Related Topics,* 278–283, 1984.

59. H. Thiemann, N. Singh, and R. W. Schunk, High frequency turbulence in a plasma driven by a current sheet, Proceedings of the *Second Symposium on Plasma Double Layers and Related Topics,* 315–320, 1984.

60. H. Thiemann, N. Singh, and R. W. Schunk, Some features of auroral electric fields as seen in 2D numerical simulations, *Adv. Space Res., 4,* 511–514, 1984.

61. N. Singh, R. W. Schunk, and H. Thiemann, Numerical simulations of double layers and auroral electric fields, *Adv. Space Res., 4,* 481–490, 1984.

62. R. W. Schunk, A. R. Barakat, H. Carlson, J. B. Evans, J. Foster, R. Greenwald, M. C. Kelley, T. Potemra, M. H. Rees, A. D. Richmond, and R. G. Noble, Assessment of plasma transport and convection at high latitudes, in, "Solar Terrestrial Physics – Present and Future," Chapter 11, 36 pages, *NASA Reference Publication, 1120*, 1984.

63. N. Singh, J. R. Conrad, and R. W. Schunk, Electrostatic ion cyclotron, beam-plasma, and lower hybrid waves excited by an electron beam, *J. Geophys. Res., 90*, 5159–5172, 1985.

64. J. J. Sojka and R. W. Schunk, A theoretical study of the global *F* region for June solstice, solar maximum, and low magnetic activity, *J. Geophys. Res., 90*, 5285–5298, 1985.

65. N. Singh, H. Thiemann, and R. W. Schunk, Dynamical features and electric field strengths of double layers driven by currents, *J. Geophys. Res., 90*, 5173–5186, 1985.

66. M. O. Chandler, R. A. Behnke, A. F. Nagy, E. G. Fontheim, P. G. Richards, and D. G. Torr, Comparison of measured and calculated low-latitude ionospheric properties, *J. Geophys. Res., 88*, 9187–9196, 1983.

67. N. Singh and R. W. Schunk, A possible mechanism for the observed streaming of O^+ and H^+ ions at nearly equal speeds in the distant magnetotail, *J. Geophys. Res., 90*, 6361–6369, 1985.

68. N. Singh and R. W. Schunk, Temporal behavior of density perturbations in the polar wind, *J. Geophys. Res., 90*, 6487–6496, 1985.

69. J. J. Sojka and R. W. Schunk, Theoretical study of anomalously high *F* region peak altitudes in the polar ionosphere, *J. Geophys. Res., 90*, 7525–7532, 1985.

70. N. Singh, J. R. Conrad, and R. W. Schunk, Electrostatic ion cyclotron waves in a plasma with an ion beam and counterstreaming bulk electrons: Waves in the zero-frequency band, *J. Geophys. Res., 90*, 12,219–12,229, 1985.

71. J. J. Sojka and R. W. Schunk, Problems with deducing ionospheric plasma convection patterns, *J. Geophys. Res., 91*, 259–269, 1986.

72. J. J. Sojka and R. W. Schunk, A theoretical study of the production and decay of localized electron density enhancements in the polar ionosphere, *J. Geophys. Res., 91*, 3245–3253, 1986.

73. P. G. Richards and D. G. Torr, An investigation of the consistency of the ionospheric measurements of the photoelectron flux and solar EUV flux, *J. Geophys. Res., 89*, 5625–5635, 1984.

74. A. F. Nagy, A. R. Barakat, and R. W. Schunk, Is Jupiter's ionosphere a significant plasma source for its magnetosphere?, *J. Geophys. Res., 91*, 351–354, 1986.

75. N. Singh, H. Thiemann, and R. W. Schunk, Numerical simulations of auroral plasma processes: Electric fields, In, "Ion Acceleration in the Magnetosphere and Ionosphere" (Editor, T. Chang), *AGU Monograph, 38*, 343–347, 1986.

76. N. Singh, H. Thiemann, and R. W. Schunk, Numerical simulations of auroral plasma processes: Ion beams and conics, In, "Ion Acceleration in the Magnetosphere and Ionosphere" (Editor, T. Chang), *AGU Monograph, 38*, 340–342, 1986.

77. N. Singh and R. W. Schunk, Ion acceleration in expanding ionospheric plasmas, In, "Ion Acceleration in the Magnetosphere and Ionosphere" (Editor, T. Chang), *AGU Monograph, 38*, 362–365, 1986.

78. C. E. Rasmussen, R. W. Schunk, and J. J. Sojka, Effects of different convection models upon the high-latitude ionosphere, *J. Geophys. Res., 91*, 6999–7005, 1986.

79. N. Singh, H. Thiemann, and R. W. Schunk, Studies on counterstreaming plasma expansion, *Physica Scripta, 33*, 355–369, 1986.

80. J. J. Sojka, C. E. Rasmussen, and R. W. Schunk, An interplanetary magnetic field dependent model of the ionospheric convection electric field, *J. Geophys. Res., 91*, 11,281–11,290, 1986.

81. N. Singh, R. W. Schunk, and H. Thiemann, Temporal features of the refilling of a plasmaspheric flux tube, *J. Geophys. Res., 91*, 13,433–13,454, 1986.

82. R. W. Schunk, J. J. Sojka, and M. D. Bowline, Theoretical study of the electron temperature in the high-latitude ionosphere for solar maximum and winter conditions, *J. Geophys. Res., 91*, 12,041–12,054, 1986.

83. H. G. Demars and R. W. Schunk, Solutions to bi-Maxwellian transport equations for SAR-arc conditions, *Planet. Space Sci., 34*, 1335–1348, 1986.

84. N. Singh, H. Thiemann, and R. W. Schunk, Plasma processes driven by current sheets and their relevance to the auroral plasma, *IEEE Transactions on Plasma Science, 14*, 805–822, 1986.

85. R. W. Schunk, An updated theory of the polar wind, *Adv. Space Res., 6*, 79–88, 1986.

86. J. J. Sojka and R. W. Schunk, Theoretical study of the high-latitude ionosphere's response to multicell convection patterns, *J. Geophys. Res., 92*, 8733–8744, 1987.

87. A. F. Nagy and R. W. Schunk, Ionosphere, In, *Encyclopedia of Physical Science and Technology, Vol. 7*, 19–33, 1987.

88. R. W. Schunk and J. J. Sojka, Ionospheric features induced by magnetospheric processes, In, *Quantitative Modeling of Magnetosphere-Ionosphere Coupling Processes*, 11–16, Kyoto Sangyo University, Japan, 1987.

89. J. J. Sojka and R. W. Schunk, Magnetospheric control of the bulk ionospheric plasma, *AGARD Conference Proceedings, 406*, 2.1–2.13, 1987.

90. N. Singh, H. Thiemann, and R. W. Schunk, Electric fields and double layers in plasmas, *Laser and Particle Beams, 5*, 233–255, 1987.

91. N. Singh, H. Thiemann, and R. W. Schunk, Simulations of auroral plasma processes: Electric fields, waves and particles, *Planet. Space Sci., 35*, 353–395, 1987.

92. J. J. Sojka, R. W. Schunk, and M. D. Bowline, Modelled ionospheric T_e profiles at mid-latitudes for possible IRI application, *Adv. Space Res., 7*, 107–110, 1987.

93. A. R. Barakat and R. W. Schunk, Stability of the polar wind, *J. Geophys. Res., 92*, 3409–3415, 1987.

94. H. G. Demars and R. W. Schunk, Comparison of solutions to bi-Maxwellian and Maxwellian transport equations for subsonic flows, *J. Geophys. Res., 92*, 5969–5990, 1987.

95. C. E. Rasmussen and R. W. Schunk, Ionospheric convection driven by NBZ currents, *J. Geophys. Res., 92*, 4491–4504, 1987.

96. R. W. Schunk, Interactions between the polar ionosphere and thermosphere, *Physica Scripta, T18*, 256–275, 1987.

97. R. W. Schunk, J. J. Sojka, and M. D. Bowline, Theoretical study of the effect of ionospheric return currents on the electron temperature, *J. Geophys. Res., 92*, 6013–6022, 1987.

98. H. G. Demars and R. W. Schunk, Temperature anisotropies in the terrestrial ionosphere and plasmasphere, *Rev. Geophys., 25*, 1659–1679, 1987.

99. A. R. Barakat, R. W. Schunk, T. E. Moore, and J. H. Waite, Jr., Ion escape fluxes from the terrestrial high-latitude ionosphere, *J. Geophys. Res., 92*, 12,255–12,266, 1987.

100. H. Thiemann, R. W. Schunk, N. Singh, and R. Grard, Giotto-spacecraft charging due to impact generated plasma in the presence of dielectric materials, *AGARD Conference Proceedings, 406*, 11.1–11.7, 1987.

101. R. W. Schunk and J. J. Sojka, A theoretical study of the lifetime and transport of large ionospheric density structures, *J. Geophys. Res., 92*, 12,343–12,351, 1987.

102. N. Singh, U. Samir, K. H. Write, and N. H. Stone, A possible explanation of the electron temperature enhancement in the wake of a satellite, *J. Geophys. Res., 92*, 6100–6111, 1987.

103. J. J. Sojka and R. W. Schunk, A model study of how electric field structures affect the polar cap *F* region, *J. Geophys. Res., 93*, 884–896, 1988.

104. R. J. Sica, R. W. Schunk, and C. E. Rasmussen, Can the high latitude ionosphere support large field-aligned ion drifts?, *J. Atmos. Terr. Phys., 50*, 141–152, 1988.

105. A. R. Barakat, R. W. Schunk, T. E. Moore, and J. H. Waite, Jr., O^+ and H^+ escape fluxes from the polar regions, In, "Modeling Magnetospheric Plasma," (Editors, T. E. Moore and J. H. Waite), *AGU Geophysical Monograph, 44*, 241–245, 1988.

106. R. W. Schunk, The polar wind, In, "Modeling Magnetospheric Plasma," (Editors, T. E. Moore and J. H. Waite), *AGU Geophysical Monograph, 44*, 219–228, 1988.

107. R. W. Schunk and E. P. Szuszczewicz, First-principle and empirical modelling of the global-scale ionosphere, *Ann. Geophysicae, 6*, 19–30, 1988.

108. E. P. Szuszczewicz, B. Fejer, E. Roelof, R. W. Schunk, R. Wolf, R. Leitinger, M. Abdu, B. M Reddy, J. Joselyn, P. Wilkinson, and R. Woodman, SUNDIAL: A worldwide study of interactive ionospheric processes and their roles in the transfer of energy and mass in the sun-earth system, *Ann. Geophysicae, 6*, 3–18, 1988.

109. R. W. Schunk, A mathematical model of the middle and high latitude ionosphere, *PAGEOPH, 127*, 255–303, 1988.

110. C. E. Rasmussen, J. J. Sojka, R. W. Schunk, V. B. Wickwar, O. de la Beaujardiere, J. Foster, and J. Holt, Comparison of simultaneous Chatanika and

Millstone Hill temperature measurements with ionospheric model predictions, *J. Geophys. Res., 93*, 1922–1932, 1988.

111. C. E. Rasmussen, R. W. Schunk, and V. B. Wickwar, A photochemical equilibrium model for ionospheric conductivity, *J. Geophys. Res., 93*, 9831–9840, 1988.

112. R. W. Schunk and J. J. Sojka, Ionospheric climate and weather modeling, *EOS, 69*, 153–165, 1988.

113. T. I. Gombosi and R. W. Schunk, A comparative study of plasma expansion events in the polar wind, *Planet. Space Sci., 36*, 753–764, 1988.

114. E. P. Szuszczewicz, B. Fejer, R. W. Schunk, E. Roelof, R. Wolf, SUNDIAL: An international program in solar-terrestrial physics, *WITS Handbook, Vol. 1*, 208–213, (Editors, C. H. Liu and B. Edwards), SCOSTEP, 1988.

115. C. E. Rasmussen and R. W. Schunk, Multistream hydrodynamic modeling of interhemispheric plasma flow, *J. Geophys. Res., 93*, 14,557–14,565, 1988.

116. C. E. Rasmussen and R. W. Schunk, Ionospheric convection inferred from interplanetary magnetic field-dependent Birkeland currents, *J. Geophys. Res., 93*, 1909–1921, 1988.

117. J. A. Klimchuk, P. A. Sturrock, and W.-H. Yang, Coronal magnetic fields produced by photospheric shear, *Astrophys. J., 335*, 456–467, 1988.

118. W.-H. Yang and R. W. Schunk, Discrete events and solar wind energization, *Ap. J., 343*, 494–498, 1989.

119. R. W. Schunk and J. J. Sojka, Modelling ionospheric density structures, AGARD/NATO Symposium on, "Ionospheric Structure and Variability on a Global Scale and Interactions With Atmosphere and Magnetosphere," *Conference Proceedings, 441*, 14.1–14.12, 1989.

120. H. G. Demars and R. W. Schunk, Solutions to bi-Maxwellian transport equations for the polar wind, *Planet. Space Sci., 37*, 85–96, 1989.

121. R. W. Schunk, Polar wind theory, In, "Physics of Space Plasmas," *SPI Conf. Proc. and Reprint Series, 7*, 183–202, 1987.

122. E. P. Szuszczewicz, R. A. Wolf, R. W. Spiro, B. G. Fejer, R. W. Schunk, and E. Roelof, Ionospheric responses to coupling processes in the solar-terrestrial system: SUNDIAL perspectives, In, "Physics of Space Plasmas," *SPI Conf. Proc. and Reprint Series, 7*, 215–225, 1988.

123. A. R. Barakat and R. W. Schunk, Stability of H^+ beams in the polar wind, *J. Geophys. Res., 94*, 1487–1494, 1989.

124. H. Thiemann, R. W. Schunk, and R. Zwickl, Dynamic PIC-simulations of charging phenomena related to the ICE-spacecraft in both cometary and solar wind environments, *Adv. Space Res., 9*, 389–392, 1989.

125. R. W. Schunk, Polar wind tutorial, In, "Physics of Space Plasmas," *SPI Conf. Proc. and Reprint Series, 8*, 81–134, 1988.

126. J. J. Sojka and R. W. Schunk, Theoretical study of the seasonal behavior of the global ionosphere at solar maximum, *J. Geophys. Res., 94*, 6739–6749, 1989.

127. R. W. Schunk, Response of the ionosphere–thermosphere system to magnetospheric forcing, *Adv. Space Res., 10*, 133–142, 1990.

128. W.-H. Yang, Expansion of solar-terrestrial low-β plasmoid, *Astrophys. J.*, in press.

129. R. W. Schunk, Magnetosphere-ionosphere-thermosphere coupling processes, (STEP), *STEP Handbook*, 52–110, 1988.

130. R. W. Schunk and J. J. Sojka, A three-dimensional time-dependent model of the polar wind, *J. Geophys. Res., 94*, 8973–8991, 1989.

131. H. G. Demars and R. W. Schunk, Solutions to bi-Maxwellian transport equations for radial solar wind beyond 28 R_S, *Planet. Space Sci., 39*, 435–451, 1991.

132. C. E. Rasmussen and R. W. Schunk, A three-dimensional time-dependent model of the plasmasphere, *J. Geophys. Res., 95*, 6133–6144, 1990.

133. J. J. Sojka, Global scale, physical models of the *F*-region ionosphere, *Rev. Geophys., 27*, 371–403, 1989.

134. T.-Z. Ma and R. W. Schunk, A two-dimensional model of plasma expansion in the ionosphere, *Planet. Space Sci., 38*, 723–741, 1990.

135. H. G. Demars and R. W. Schunk, Solar wind proton velocity distributions: Comparison of bi-Maxwellian based 16-moment expansion with observations, *Planet. Space Sci., 38*, 1091–1103, 1990.

Cumulative STTP Presentations

1. *R. W. Schunk*, W. J. Raitt, and J. J. Sojka, A theoretical study of the high-latitude winter *F*-region at solar minimum for low magnetic activity, AGU Fall Meeting, San Francisco, California; *EOS, 61*, 1059, 1980.

2. *W. J. Raitt*, R. W. Schunk, and J. J. Sojka, Theoretical predictions for ion composition in the high-latitude winter *F*-region for solar minimum and low magnetic activity, AGU Fall Meeting, San Francisco, California; *EOS, 61*, 1059, 1980.

3. *D. S. Watkins* and R. W. Schunk, Electron temperature anistropy in the polar wind, AGU Fall Meeting, San Francisco, California; *EOS, 61*, 1092, 1980.

4. *R. W. Schunk*, W. J. Raitt, and J. J. Sojka, High-latitude ionospheric model: First step towards a predictive capability, presented at the symposium on the *Effect of the Ionosphere on Radiowave Systems*, April 14–16, 1981; Alexandria, Virgina.

5. *R. W. Schunk*, Theoretical models of high-latitude electrodynamics, *Invited Review*, 4th IAGA Scientific Assembly, August 3–15, Edinburgh, Scotland; *IAGA Bulletin, 45*, 289, 1981.

6. *R. W. Schunk*, Ionospheric dynamics, *Invited Review*, Thermosphere Workshop, October 19–21, 1981; NASA Goddard Space Flight Center, Greenbelt, Maryland.

7. *R. W. Schunk*, The flow of plasma in the solar terrestrial environment, *Invited Review*, AGU Fall Meeting, San Francisco, California; *EOS, 62*, 1016, 1981.

8. D. S. Watkins and *R. W. Schunk*, Proton temperature anistropy in the polar wind, AGU Fall Meeting, San Francisco, California; *EOS, 62*, 1012, 1981.

9. *N. Singh* and R. W. Schunk, Double layer motion, AGU Fall Meeting, San Francisco, California; *EOS, 62*, 1011, 1981.

10. *J. J. Sojka*, J. C. Foster, P. M. Banks, and J. R. Doupnik, Mapping electrostatic potentials from the ionosphere to the inner magnetosphere, AGU Fall Meeting, San Francisco, California; *EOS, 62*, 1012, 1981.

11. *R. W. Schunk*, J. J. Sojka, and W. J. Raitt, Seasonal variations of the high-latitude *F* region for strong convection, AGU Fall Meeting, San Francisco, California; *EOS, 62*, 1011, 1981.

12. *J.-P. St.-Maurice* and R. W. Schunk, Ion-neutral momentum coupling near discrete high-latitude ionospheric features, AGU Fall Meeting, San Francisco, California; *EOS, 62*, 1011, 1981.

13. *P. G. Richards* and D. G. Torr, Determination of photoionization branching ratios at 304 Å from experimental ionospheric photoelectron fluxes, AGU Fall Meeting, San Francisco, California; *EOS, 62*, 1013, 1981.

14. *R. W. Schunk*, The polar wind: A source of magnetospheric plasma, *Invited Review*, presented at the "Conference on Origins of Plasmas and Electric Fields in the Magnetosphere," January 25–29, 1982; Yosemite, California.

15. N. Singh and *R. W. Schunk*, Current carrying properties of double layers and low frequency auroral fluctuations, presented at the "Conference on Origins of Plasma and Electric Fields in the Magnetosphere," January 25–29, 1982; Yosemite, California.

16. *J. J. Sojka* and R. W. Schunk, The polar *F*-region response to a magnetospheric storm, COSPAR, 24th Plenary Meeting, May 16–June 2, 1982; Ottawa, Ontario, Canada.

17. *H. Thiemann*, N. Singh, and R. W. Schunk, Numerical simulations of V-shaped potential structures, AGU Spring Meeting, Baltimore, Maryland; *EOS, 63*, 582, 1982.

18. *R. W. Schunk*, The terrestrial ionosphere, five one-hour lectures presented at the "Theory Institute in Solar-Terrestrial Physics," August 9–26, 1982; Boston College, Massachusetts.

19. *N. Singh* and R. W. Schunk, Dynamical features of moving double layers, presented at the "Theory Institute in Solar-Terrestrial Physics," August 9–26, 1982; Boston College, Massachusetts.

20. *J. J. Sojka* and R. W. Schunk, The response of the high latitude *F*-region to an idealized magnetospheric storm, presented at the "Theory Institute in Solar-Terrestrial Physics," August 9–26, 1982; Boston College, Massachusetts.

21. N. Singh and *R. W. Schunk*, Numerical calculations relevant to the initial expansion of the polar wind, presented at the "Theory Institute in Solar-Terrestrial Physics," August 9–26, 1982; Boston College, Massachusetts.

22. *N. Singh*, R. W. Schunk, and J. J. Sojka, Stochastic acceleration of ionospheric ions by a coherent wave, presented at the "Theory Institute in Solar-Terrestrial Physics," August 9–26, 1982; Boston College, Massachusetts.

23. *J. H. Waite*, J. F. E. Johnson, J. L. Green, C. R. Chappell, J. J. Sojka, and R. W. Schunk, Polar ion streams, AGU Fall Meeting, San Francisco, California; *EOS, 63*, 1073, 1982.

24. *R. W. Schunk,* High-latitude ionospheric dynamics, *Invited Talk,* presented at the "MITHRAS Workshop," February 7–8, 1983; Boulder, Colorado.

25. *R. W. Schunk,* Ionospheric studies using the incoherent scatter chain of radars, *Invited Talk,* presented at the "Second NSF Workshop on the Incoherent Scatter Radar Database," February 9–10, 1983; Boulder, Colorado.

26. *J. J. Sojka,* R. W. Schunk, J. V. Evans, J. M. Holt, and R. Wand, Comparison of model high-latitude electron densities with Millstone Hill observations, AGU Spring Meeting, Baltimore, Maryland; *EOS, 64,* 278, 1983.

27. *R. W. Schunk,* Electrodynamics of the high latitude ionosphere, *Invited Review,* IAGA Scientific Assembly, August 15–27, Hamburg, Germany; *IAGA Bulletin, 48,* 282, 1983.

28. *J. J. Sojka* and R. W. Schunk, Pertinent characteristics of the topside ionosphere in its role as a source of magnetospheric plasma, *Invited Talk,* IAGA Scientific Assembly, August 15–27, Hamburg, Germany; *IAGA Bulletin, 48,* 323, 1983.

29. *P. G. Richards,* D. G. Torr, and R. W. Schunk, The applicability of the low speed formulation to the refilling of magnetic flux tubes, IAGA Scientific Assembly, August 15–27, Hamburg, Germany; *IAGA Bulletin, 48,* 324, 1983.

30. *R. W. Schunk,* Polar cap models, *Invited Review,* presented at the AFGL Polar Cap Workshop, October 18–20, 1983; Bedford, Massachusetts.

31. *R. W. Schunk,* Plasmapause signatures in the ionosphere, *Invited Review,* presented at the conference on "Fundamental Magnetospheric Processes in the Plasmapause Region," October 26–27, 1983; MSFC, Huntsville, Alabama.

32. *N. Singh* and R. W. Schunk, Numerical simulations of counterstreaming plasmas and their relevance to interhemispheric flows, presented at the conference on "Fundamental Magnetospheric Processes in the Plasmapause Region," October 26–27, 1983; MSFC, Huntsville, Alabama.

33. *J. J. Sojka* and R. W. Schunk, The global ionosphere for quiet conditions: A model study, AGU Fall Meeting, San Francisco, California; *EOS, 64,* 777, 1983.

34. *R. W. Schunk* and J. J. Sojka, Problems with deducing plasma convection patterns from multiple radar observations, AGU Fall Meeting, San Francisco, California; *EOS, 64,* 777, 1983.

35. *A. R. Barakat* and R. W. Schunk, O^+ ions in the polar wind, AGU Fall Meeting, San Francisco, California; *EOS, 64,* 778, 1983.

36. *N. Singh* and R. W. Schunk, Energization of ions in the auroral plasma by broadband waves, AGU Fall Meeting, San Francisco, California; *EOS, 64,* 797, 1983.

37. J. R. Conrad, *N. Singh,* and R. W. Schunk, Electrostatic ion cyclotron waves in a multi-ion plasma driven by an electron current, AGU Fall Meeting, San Francisco, California; *EOS, 64,* 811, 1983.

38. *H. Thiemann,* N. Singh, and R. W. Schunk, Fluctuations of V-shaped potential structures in a magnetized plasma, AGU Fall Meeting, San Francisco, California; *EOS, 64,* 811, 1983.

39. *R. W. Schunk,* A global ionospheric model, *Invited Review,* presented at the Optical Ground-Based Aeronomy Workshop II, June 20–22, 1984; Ann Arbor, Michigan.

40. *R. W. Schunk,* A global ionospheric model, and also Comparison of ionospheric model predictions with incoherent scatter radar observations, two one-hour lectures presented at the Arecibo Observatory, July 16–18, 1984; Arecibo, Puerto Rico.

41. *N. Singh* and R. W. Schunk, The relationship between the electric fields associated with plasma expansion and double layers, presented at the Second Double Layer Symposium and Related Topics, July 5–6, 1984; Innsbruck, Austria.

42. *N. Singh* and R. W. Schunk, Can Buneman double layers be driven in auroral plasmas?, presented at the Second Double Layer Symposium and Related Topics, July 5–6, 1984; Innsbruck, Austria.

43. *N. Singh,* H. Thiemann, and R. W. Schunk, Current fluctuations and dynamical features of double layer potential profiles, presented at the Second Double Layer Symposium and Related Topics, July 5–6, 1984; Innsbruck, Austria.

44. *N. Singh,* H. Thiemann, and R. W. Schunk, Numerical simulations of double layers and auroral electric fields, *Invited Review,* COSPAR, 25th Plenary Meeting, June 30–July 2, 1984; Graz, Austria.

45. *H. Thiemann,* N. Singh, and R. W. Schunk, Some features of auroral electric fields as seen in 2-D numerical simulations, COSPAR, 25th Plenary Meeting, June 30–July 2, 1984; Graz, Austria.

46. *R. W. Schunk,* Thermospheric structure and circulation in the polar cap, *Invited Review,* presented at the Chapman Conference on the Magnetospheric Polar Cap, August 6–9, 1984; Fairbanks, Alaska.

47. *R. W. Schunk,* High latitude ionospheric predictions, presented at the GISMOS Workshop, October 24–26, 1984; Boulder, Colorado.

48. *R. W. Schunk,* Global models of ionospheric parameters, presented at the GISMOS Workshop, October 24–26, 1984; Boulder, Colorado.

49. *R. W. Schunk,* Ionosphere-magnetosphere coupling, *Invited Talk,* presented at the Solar-Terrestrial Theory Program Meeting/Workshop, November 14–16, 1984; Los Alamos, New Mexico.

50. *R. W. Schunk* and J. J. Sojka, Critical tests of a global ionospheric model, *Invited Talk,* AGU Fall Meeting, San Francisco, California; *EOS, 65,* 1026, 1984.

51. *R. W. Schunk,* The flow of plasma in the solar-terrestrial system, *Colloquium,* Department of Physics and Astronomy, Brigham Young University, January 9, 1985; Provo, Utah.

52. *N. Singh,* H. Thiemann, and R. W. Schunk, Electric fields in 2-D double layer simulations and their comparison with satellite observations, presented at the 2nd International School for Space Simulation, February 4–15, 1985; Kauai, Hawaii.

53. *N. Singh* and R. W. Schunk, Temporal behavior of density perturbations in the polar wind, presented at the 2nd International School for Space Simulation, February 4–15, 1985; Kauai, Hawaii.

54. *C. E. Rasmussen,* R. W. Schunk, and J. J. Sojka, Modeling of the polar ionosphere, presented at the 2nd International School for Space Simulation, February 4–15, 1985; Kauai, Hawaii.

55. *A. R. Barakat* and R. W. Schunk, Effect of hot electrons on the polar wind, presented at the 2nd International School for Space Simulation, February 4–15, 1985; Kauai, Hawaii.

56. J. J. Sojka and *R. W. Schunk,* A theoretical study of the global *F* region for June solstice and low magnetic activity, presented at the 2nd International School for Space Simulation, February 4–15, 1985; Kauai, Hawaii.

57. *N. Singh,* H. Thiemann, and R. W. Schunk, Ion conics as seen in simulations of 2-D potential structures, presented at the Chapman Conference on Ion Acceleration in the Magnetosphere and Ionosphere, June 3–7, 1985; Wellesley, Massachusetts.

58. *N. Singh* and R. W. Schunk, Ion acceleration in expanding ionospheric plasmas, presented at the Chapman Conference on Ion Acceleration in the Magnetosphere and Ionosphere, June 3–7, 1985; Wellesley, Massachusetts.

59. N. Singh, *H. Thiemann,* and R. W. Schunk, Ion beams as seen in simulations of 2-D potential structures, presented at the Chapman Conference on Ion Acceleration in the Magnetosphere and Ionosphere, June 3–7, 1985; Wellesley, Massachusetts.

60. *N. Singh* and R. W. Schunk, A possible mechanism for the observed streaming of O^+ and H^+ ions at nearly equal speeds in the distant magnetotail, presented at the Chapman Conference on Ion Acceleration in the Magnetosphere and Ionosphere, June 3–7, 1985; Wellesley, Massachusetts.

61. *R. W. Schunk* and J. J. Sojka, A model of the global ionosphere, *Invited Review,* presented at the 1985 North American Radio Science Meeting, June 17–21, 1985; Vancouver, British Columbia, Canada.

62. *J. J. Sojka* and R. W. Schunk, Theoretical study of the production and decay of localized electron density enhancements in the polar ionosphere, presented at the 1985 North American Radio Science Meeting, June 17–21, 1985; Vancouver, British Columbia, Canada.

63. *J. J. Sojka* and R. W. Schunk, Theoretical study of anomalously high *F*-region peak altitudes in the polar ionosphere, presented at the 1985 North American Radio Science Meeting, June 17–21, 1985; Vancouver, British Columbia, Canada.

64. C. E. Rasmussen, R. W. Schunk, J. J. Sojka, *V. B. Wickwar,* O. de la Beaujardiere, J. C. Foster, J. Holt, D. S. Evans, and E. Nielsen, Comparison of simultaneous Chatanika and Millstone Hill observations with ionospheric model predictions, AGU Spring Meeting, Baltimore, Maryland; *EOS, 66,* 327, 1985.

65. *N. Singh,* A review of mechanisms for the formation of ion conics, *Invited Review,* 5th IAGA Scientific Assembly, August 5–17, 1985; Prague, Czechoslovakia.

66. *R. W. Schunk,* Models of the terrestrial high latitude ionosphere, *Invited Review,* 5th IAGA Scientific Assembly, August 5–17, 1985; Prague, Czechoslovakia.

67. *A. R. Barakat,* R. W. Schunk, T. E. Moore, and J. H. Waite, Ion escape fluxes in the terrestrial high latitude ionosphere, 5th IAGA Scientific Assembly, August 5–17, 1985; Prague, Czechoslovakia.

68. A. F. Nagy, *A. R. Barakat* and R. W. Schunk, Is Jupiter's ionosphere a significant plasma source for its magnetosphere?, 5th IAGA Scientific Assembly, August 5–17, 1985; Prague, Czechoslovakia.

69. *H. Thiemann,* N. Singh, and R. W. Schunk, Simulation of auroral potential structures and related phenomena, 5th IAGA Scientific Assembly, August 5–17, 1985; Prague, Czechoslovakia.

70. *R. W. Schunk,* Comparison of transport equations for gases and plasmas, and also Convergence of the transport equations for gases and plasmas, two one-hour lectures presented at the Institut für Astrophysik und Extraterrestrische Forschung, Universität Bonn, August 15–16, 1985; Bonn, West Germany.

71. *N. Singh,* Counterstreaming plasma expansion, *Invited Lecture,* presented at the Nordic Nonlinear Plasma Wave Meeting, Risø National Laboratory, August 13–16, 1985; Risø, Denmark.

72. *N. Singh,* Simulation of auroral plasma processes, presented at the Department of Electron and Plasma Physics, Royal Institute of Technology, August 21, 1985; Stockholm, Sweden.

73. *R. W. Schunk,* A theoretical global ionospheric *F*-region model and its predictive aspects, *Invited Lecture,* presented at the SUNDIAL Workshop, September 24–26, 1985; McLean, Virginia.

74. *R. W. Schunk* and J. J. Sojka, Magnetospheric control of ionospheric processes, *Invited Review,* AGU Fall Meeting, San Francisco, California; *EOS, 66,* 995, 1985.

75. *J. J. Sojka* and R. W. Schunk, Ionospheric modelling of the GISMOS campaign, *Invited Talk,* AGU Fall Meeting, San Francisco, California; *EOS, 66,* 994, 1985.

76. *C. E. Rasmussen,* R. W. Schunk, and J. J. Sojka, Effects of different convection models upon the high-latitude ionosphere, AGU Fall Meeting, San Francisco, California; *EOS, 66,* 996, 1985.

77. *M. D. Bowline,* R. W. Schunk, and J. J. Sojka, Theoretical study of the electron temperature in the high latitude ionosphere for solar maximum and winter conditions, AGU Fall Meeting, San Francisco, California; *EOS, 66,* 999, 1985.

78. J. R. Conrad, *N. Singh,* and R. W. Schunk, EIC waves in a plasma with an ion beam and counterstreaming bulk electrons: Waves in the zero-frequency band, AGU Fall Meeting, San Francisco, California; *EOS, 66,* 1034, 1985.

79. *N. Singh,* R. W. Schunk, and H. Thiemann, Temporal features of the refilling of a plasmaspheric flux tube, AGU Fall Meeting, San Francisco, California; *EOS, 66,* 1036, 1985.

80. H. Thiemann, *N. Singh,* and R. W. Schunk, Numerical simulations of auroral plasma processes, AGU Fall Meeting, San Francisco, California; *EOS, 66,* 1050, 1985.

81. D. G. Torr, R. W. Schunk, *T. L. Killeen,* and R. G. Roble, The role of thermosphere/ionosphere modeling for the GBOA–CEDAR initiative, *Invited Talk*, AGU Fall Meeting, San Francisco, California; *EOS, 66,* 990, 1985.

82. N. Singh and *R. W. Schunk,* Plasma response to the injection of an electron beam, *Invited Talk*, National Radio Science Meeting, January 13–16, 1986; Boulder, Colorado.

83. *R. W. Schunk,* Round Table Discussion on Global Ionosphere and Aeronomy Study Program, *Invited Participant,* National Radio Science Meeting, January 13–16, 1986; Boulder, Colorado.

84. *R. W. Schunk,* Space science: High technology now and in the future, *Invited Lecture*, Business and Professional Women's Organization, April 21, 1986; Logan, Utah.

85. *R. W. Schunk,* Solar-terrestrial physics: A space age birth, *73rd Faculty Honor Lecture*, Utah State University, May 1, 1986; Logan, Utah.

86. *R. W. Schunk,* Solar-terrestrial physics, *Colloquium*, Department of Physics, University of Utah, May 8, 1986; Salt Lake City, Utah.

87. *C. E. Rasmussen,* P. M. Banks, and R. W. Schunk, Theory of the electrodynamic tether, COSPAR, 26th Plenary Meeting, June 30–July 11, 1986; Toulouse, France.

88. *H. Thiemann,* R. Grard, N. Singh, and R. W. Schunk, Results of model calculations simulating the interaction between the Giotto spacecraft and the impact induced secondary plasma, COSPAR, 26th Plenary Meeting, June 30–July 11, 1986; Toulouse, France.

89. *J. J. Sojka,* R. W. Schunk, and M. D. Bowline, Modelled ionospheric T_e profiles at high latitudes for possible IRI application, COSPAR, 26th Plenary Meeting, June 30–July 11, 1986; Toulouse, France.

90. *R. W. Schunk,* An updated theory of the polar wind, *Invited Review*, COSPAR, 26th Plenary Meeting, June 30–July 11, 1986; Toulouse, France.

91. *E. P. Szuszczewicz,* E. Roelof, R. W. Schunk, B. Fejer, R. Wolf, R. Leitinger, M. Abdu, B. M. Reddy, J. Joselyn, P. J. Wilkinson, and R. F. Woodman, A cooperative world-wide study of interactive ionospheric processes and their role in the transfer of energy and mass in the Sun-Earth system; SCOSTEP International Symposium on Solar-Terrestrial Physics, June 30–July 5, 1986; Toulouse, France.

92. *J. J. Sojka,* R. W. Schunk, L. A. Frank, J. D. Craven, J. D. Winningham, and J. R. Sharber, Ionosphere's response to an auroral storm based upon the Dynamics Explorer SAI and LAPI data bases, SCOSTEP International Symposium on Solar-Terrestrial Physics, June 30–July 5, 1986; Toulouse, France.

93. *R. W. Schunk,* Interactions between the polar ionosphere and thermosphere, *Invited Review*, SCOSTEP International Symposium on Solar-Terrestrial Physics, June 30–July 5, 1986; Toulouse, France.

94. *R. W. Schunk,* The polar wind, *Invited Review*, presented at The First Huntsville Workshop on Magnetosphere-Ionosphere Plasma Models, October 13–16, 1986; Huntsville, Alabama.

95. *A. R. Barakat,* R. W. Schunk, T. E. Moore and J. H. Waite, Ion escape fluxes in the terrestrial high latitude ionosphere, presented at The First Huntsville Workshop on Magnetosphere Ionosphere Plasma Models, October 13–16, 1986; Huntsville, Alabama.

96. *R. W. Schunk,* Ionosphere-thermosphere modelling: Current status, *Invited Review*, presented at the International Symposium on Large-Scale Processes in the Ionospheric-Thermospheric System, December 2–5, 1986; Boulder, Colorado.

97. *C. E. Rasmussen,* R. W. Schunk, J. J. Sojka, V. B. Wickwar, O. de la Beaujardiere, J. C. Foster, and J. M. Holt, Comparison of simultaneous Chatanika and Millstone Hill temperature measurements with ionospheric model predictions, presented at the International Symposium on Large-Scale Processes in the Ionospheric-Thermospheric System, December 2–5, 1986; Boulder, Colorado.

98. *J. J. Sojka* and R. W. Schunk, Asymmetries in the plasma characteristics of the conjugate high-latitude ionospheres, presented at the International Symposium on Large-Scale Processes in the Ionospheric-Thermospheric System, December 2–5, 1986; Boulder, Colorado.

99. *C. E. Rasmussen* and R. W. Schunk, An *E* and *F* region density model for obtaining ionospheric conductivity, presented at the International Symposium on Large-Scale Processes in the Ionospheric-Thermospheric System, December 2–5, 1986; Boulder, Colorado.

100. *E. P. Szuszczewicz,* E. C. Roelof, R. W. Schunk, B. G. Fejer, R. A. Wolf, R. Leitinger, M. A. Abdu, B. M. Reddy, J. C. Joselyn, P. J. Wilkinson, and R. F. Woodman, SUNDIAL: A continuing program of global-scale modeling and measurement of ionospheric responses to solar, magnetospheric, and thermospheric controls, presented at the International Symposium on Large-Scale Processes in the Ionospheric-Thermospheric System, December 2–5, 1986; Boulder, Colorado.

101. *R. W. Schunk,* Ionospheric physics: The impact of plasma transport, *Invited Talk,* AGU Fall Meeting, San Francisco, California; *EOS, 67,* 1126, 1986.

102. *H. G. Demars* and R. W. Schunk, Comparison of solutions to bi-Maxwellian and Maxwellian transport equations for subsonic flows, AGU Fall Meeting, San Francisco, California; *EOS, 67,* 1136, 1986.

103. *A. R. Barakat* and R. W. Schunk, Stability of the polar wind, AGU Fall Meeting, San Francisco, California; *EOS, 67,* 1136, 1986.

104. *J. J. Sojka* and R. W. Schunk, Theoretical study of the high latitude ionosphere's response to multi-cell convection patterns, AGU Fall Meeting, San Francisco, California; *EOS, 67,* 1137, 1986.

105. *R. J. Sica,* C. E. Rasmussen, and R. W. Schunk, Can the high latitude ionosphere support large field-aligned ion drifts?, AGU Fall Meeting, San Francisco, California; *EOS, 67,* 1137, 1986.

106. *R. W. Schunk* and J. J. Sojka, The lifetime and transport of severe ionospheric disturbances, AGU Fall Meeting, San Francisco, California; *EOS, 67,* 1137, 1986.

107. *C. E. Rasmussen* and R. W. Schunk, Ionospheric convection driven by NBZ currents, AGU Fall Meeting, San Francisco, California; *EOS, 67,* 1162, 1986.

108. *C. E. Rasmussen* and R. W. Schunk, Ionospheric convection driven by asymmetries in NBZ currents, National Radio Science Meeting, January 12–15, 1987; Boulder, Colorado.

109. *R. W. Schunk,* Implications of the SUNDIAL data on first-principles global-scale models, presented at the Third SUNDIAL Workshop, February 24–27, 1987; La Jolla, California.

110. *R. W. Schunk* and J. J. Sojka, Ionospheric features induced by magnetospheric processes, *Invited Talk,* presented at the International Symposium on Quantitative Modeling of Magnetosphere-Ionosphere Coupling Processes, March 9–13, 1987; Kyoto, Japan.

111. *E. P. Szuszczewicz,* E. Roelof, R. W. Schunk, B. Fejer, R. Wolf, M. Abdu, J. Joselyn, B. M. Reddy, P. Wilkinson, R. Woodman, and R. Leitinger, SUNDIAL: A global study of ionospheric processes and their roles in the transfer of energy and mass in the sun-earth system, AGU Spring Meeting, Baltimore, Maryland; *EOS, 68,* 364, 1987.

112. *R. W. Schunk* and E. P. Szuszczewicz, First-principle and empirical modeling of the global-scale ionosphere, *Invited Talk*, AGU Spring Meeting, Baltimore, Maryland; *EOS, 68*, 364, 1987.

113. P. J. Wilkinson, *R. W. Schunk,* R. Hanbaba, and E. P. Szuszczewicz, Interhemispheric comparison of SUNDIAL *F*-region data with global-scale ionospheric models, AGU Spring Meeting, Baltimore, Maryland; *EOS, 68*, 364, 1987.

114. *M. A. Abdu,* B. M. Reddy, G. O. Walker, R. Hanbaba, J. H. A. Sobral, B. G. Fejer, R. W. Schunk, R. F. Woodman, and E. P. Szuszczewicz, Processes in the quiet and disturbed equatorial low latitude ionosphere: SUNDIAL campaign 1984, AGU Spring Meeting, Baltimore, Maryland; *EOS, 68*, 364, 1987.

115. *R. W. Schunk,* Polar wind theory, *Invited Review*, presented at the 1987 Cambridge Workshop in Theoretical Geoplasma Physics on "Ionosphere-Magnetosphere-Solar Wind Coupling Processes," July 28–August 1, 1987; Cambridge, Massachusetts.

116. *R. W. Schunk* and E. P. Szuszczewicz, First-principal and empirical modelling of the global-scale ionosphere, presented at the International Union of Geodesy and Geophysics, August 9–22, 1987; Vancouver, British Columbia, Canada.

117. *R. J. Sica,* C. E. Rasmussen, and R. W. Schunk, Can the high-latitude ionosphere support large field-aligned ion drifts?, presented at the International Union of Geodesy and Geophysics, August 9–22, 1987; Vancouver, British Columbia, Canada.

118. *C. E. Rasmussen* and R. W. Schunk, Ionospheric convection driven by NBZ currents, presented at the International Union of Geodesy and Geophysics, August 9–22, 1987; Vancouver, British Columbia, Canada.

119. *A. R. Barakat* and R. W. Schunk, Stability of the polar wind: Linear theory and simulation, presented at the International Union of Geodesy and Geophysics, August 9–22, 1987; Vancouver, British Columbia, Canada.

120. *C. E. Rasmussen* and R. W. Schunk, An *E*- and *F*-region density model for obtaining ionospheric conductivity, presented at the International Union of Geodesy and Geophysics, August 9–22, 1987; Vancouver, British Columbia, Canada.

121. *C. E. Rasmussen,* J. J. Sojka, R. W. Schunk, V. B. Wickwar, O. de la Beaujardiere, J. Foster, and J. Holt, Comparison of simultaneous Chatanika and Millstone Hill temperature measurements with ionospheric model predictions, presented at the International Union of Geodesy and Geophysics, August 9–22, 1987; Vancouver, British Columbia, Canada.

122. *J. J. Sojka,* New results in modelling the global and high latitude ionospheric dynamics, presented at the International Union of Geodesy and Geophysics, August 9–22, 1987; Vancouver, British Columbia, Canada.

123. *R. W. Schunk,* Ionosphere-thermosphere interaction modelling; Current status, *Invited Paper*, AGU Fall Meeting, San Francisco, California; *EOS, 68,* 1382, 1987.

124. *H. G. Demars* and R. W. Schunk, Temperature anisotropies in the ionosphere, AGU Fall Meeting, San Francisco, California; *EOS, 68*, 1382, 1987.

125. *J. J. Sojka* and R. W. Schunk, A model study of how electric field structures affect the polar cap *F*-region, AGU Fall Meeting, San Francisco, California; *EOS, 68*, 1385, 1987.

126. *A. R. Barakat* and R. W. Schunk, Effect of cusp H^+ and O^+ beams on the stability of the polar wind, AGU Fall Meeting, San Francisco, California; *EOS, 68*, 1386, 1987.

127. *W.-H. Yang* and R. W. Schunk, A model of solar wind streams, AGU Fall Meeting, San Francisco, California; *EOS, 68*, 1410, 1987.

128. *C. E. Rasmussen* and R. W. Schunk, Multi-fluid approach to study the refilling of plasmaspheric flux tubes, AGU Fall Meeting, San Francisco, California; *EOS, 68*, 1421, 1987.

129. J. Liu, *C. E. Rasmussen,* R. J. Sica, R. W. Schunk, and A. D. Richmond, Motion of ionospheric flux tubes during a period of substorm activity, AGU Fall Meeting, San Francisco, California; *EOS, 68*, 1430, 1987.

130. *R. W. Schunk* and J. J. Sojka, Modelling ionospheric density structures, *Invited Talk*, presented at the National Radio Science Meeting, January 5–8, 1988; Boulder, Colorado.

131. *R. W. Schunk,* A. R. Barakat, H. G. Demars, T.-Z. Ma, C. E. Rasmussen, J. J. Sojka, H. Thiemann, and W.-H. Yang, The flow of plasma in the solar-terrestrial environment, *Invited*, AGU Spring Meeting, Baltimore, Maryland; *EOS, 69*, 423, 1988.

132. *C. E. Rasmussen* and R. W. Schunk, A three-dimensional time-dependent model of the plasmasphere, AGU Spring Meeting, Baltimore, Maryland; *EOS, 69*, 428, 1988.

133. *R. W. Schunk* and J. J. Sojka, A three-dimensional time-dependent model of the polar wind, AGU Spring Meeting, Baltimore, Maryland; *EOS, 69*, 429, 1988.

134. *A. R. Barakat* and R. W. Schunk, Stability of energetic ion outflows from the ionosphere, AGU Spring Meeting, Baltimore, Maryland; *EOS, 69*, 429, 1988.

135. *J. J. Sojka* and R. W. Schunk, Modelling ionospheric density structures and dynamic auroral features, AGU Spring Meeting, Baltimore, Maryland; *EOS, 69*, 431, 1988.

136. *T.-Z. Ma* and R. W. Schunk, A two-dimensional model of plasma expansion in the ionosphere, AGU Spring Meeting, Baltimore, Maryland; *EOS, 69*, 431, 1988.

137. R. J. Sica, C. E. Rasmussen, and *R. W. Schunk,* Maximum field-aligned plasma velocities in the *F*-region, AGU Spring Meeting, Baltimore, Maryland; *EOS, 69*, 443, 1988.

138. *W.-H. Yang* and R. W. Schunk, Modelling solar wind streams and the neutral current sheet, AGU Spring Meeting, Baltimore, Maryland; *EOS, 69*, 436, 1988.

139. *R. W. Schunk* and J. J. Sojka, Modelling ionospheric density structures, AGARD Symposium on "Ionospheric Structure and Variability on a Global Scale and Interaction with Atmosphere, Magnetosphere," May 16–20, 1988; Munich, West Germany.

140. *R. W. Schunk,* Polar wind tutorial, *Invited Lecture*, presented at the 1988 Cambridge Workshop in Theoretical Geoplasma Physics on "Polar Cap Dynamics and High Latitude Ionospheric Turbulence," June 13–17, 1988; Cambridge, Massachusetts.

141. *R. W. Schunk,* Magnetosphere-ionosphere-thermosphere coupling processes, *Invited Talk*, presented at the SCOSTEP special session on "Solar-Terrestrial Energy Program (STEP): Major Scientific Problems," July 18–29, 1988; Helsinki, Finland.

142. *R. W. Schunk,* Response of the ionosphere-thermosphere system to magnetospheric forcing, *Invited Talk*, COSPAR 27th Plenary Meeting, July 18–29, 1988; Helsinki, Finland.

143. A. R. Barakat and *R. W. Schunk,* Outflow of low energy ions in the terrestrial high-latitude ionosphere, *Invited Talk*, COSPAR 27th Plenary Meeting, July 18–29, 1988; Helsinki, Finland.

144. A. R. Barakat and *R. W. Schunk,* Stability of the polar wind in the presence of cusp H^+ and O^+ ions, COSPAR 27th Plenary Meeting, July 18–29, 1988; Helsinki, Finland.

145. *H. G. Demars* and R. W. Schunk, Solutions to bi-Maxwellian transport equations for the solar wind, American Physical Society Topical Conference on Plasma Astrophysics, September 19–23, 1988; Santa Fe, New Mexico.

146. R. W. Schunk and *W.-H. Yang,* Modeling high-speed solar wind streams, American Physical Society Topical Conference on Plasma Astrophysics, September 19–23, 1988; Santa Fe, New Mexico.

147. *W.-H. Yang,* Force-free magnetic field model of accretion disk, American Physical Society Tropical Conference on Plasma Astrophysics, September 19–23, 1988; Sante Fe, New Mexico.

148. *J. A. Klimchuk,* P. A. Sturrock, and W.-H. Yang, Coronal magnetic fields produced by photospheric shear, 172nd American Astronomical Society, Kansas City, 1988.

149. *R. W. Schunk* and J. J. Sojka, Global polar wind variations during changing magnetospheric conditions, AGU Fall Meeting, San Francisco, California; *EOS, 69*, 1340, 1988.

150. *J. J. Sojka* and R. W. Schunk, Theoretical study of the seasonal behavior of the global ionosphere at solar maximum, AGU Fall Meeting, San Francisco, California; *EOS, 69*, 1349, 1988.

151. *H. G. Demars* and R. W. Schunk, Solutions to bi-Maxwellian transport equations for the solar wind, AGU Fall Meeting, San Francisco, California; *EOS, 69*, 1364, 1988.

152. *W.-H. Yang* and R. W. Schunk, Modelling high-speed solar wind streams, AGU Fall Meeting, San Francisco, California; *EOS, 69*, 1358, 1988.

153. *R. J. Sica,* R. W. Schunk, and P. Wilkinson, An empirical study of the undisturbed mid-latitude ionosphere using simultaneous, multiple site ionosonde measurements, AGU Fall Meeting, San Francisco, California; *EOS, 69*, 1350, 1988.

154. *C. E. Rasmussen* and R. W. Schunk, Comparison of plasmaspheric measurements with a three-dimensional time-dependent model of the plasmasphere, AGU Fall Meeting, San Francisco, California; *EOS, 69*, 1347, 1988.

155. *R. W. Schunk,* Modelling highly non-equilibrium space plasmas, Colloquium at the National Center for Atmospheric Research, January 5, 1989; Boulder, Colorado.

156. *R. W. Schunk,* Current status of numerical ionospheric modelling, *Invited Talk,* AGU Spring Meeting, Baltimore, Maryland, *EOS, 70*, 406, 1989.

157. *V. B. Wickwar* and R. W. Schunk, The high-latitude *F* region: Observation and theory, *Invited Talk*, presented at the Fourth EISCAT Scientific Workshop, June 5–9, 1989; Sigtuna, Sweden.

158. *J. J. Sojka,* Ionospheric physics, *Invited Talk,* Summer Institute on Atmospheric Sciences, sponsored by NASA Goddard Space Flight Center, June 21, 1989, NASA, Goddard, Greenbelt, Maryland.

159. T.-Z. Ma and *R. W. Schunk,* A 3-D model for plasma clouds in the ionosphere, IAGA Scientific Assembly, July 24–August 4, Exeter, England; *IAGA Bulletin, 53*, 393, 1989.

160. *R. W. Schunk* and E. P. Szuszczewicz, Plasma expansion phenomena: Comparison of characteristics predicted by small-scale and macroscopic formulations, IAGA Scientific Assembly, July 24–August 4, Exeter, England; *IAGA Bulletin, 53*, 393, 1989.

161. R. W. Schunk and *J. J. Sojka,* Global polar wind variations driven by magnetospheric processes, IAGA Scientific Assembly, July 24–August 4, Exeter, England; *IAGA Bulletin, 53*, 309, 1989.